

これらの変化が標的マーカーとなる。理想的な分子標的マーカーは、①特異性(癌細胞のみ認め、正常細胞には認めない)、②普遍性(すべての癌細胞に認める)、③検出(手技)が簡便容易、の条件を満たしたマーカーである。しかし、それをすべて満たす理想的マーカーは現在のところはなく、新たなマーカーの検索が現在でも行われている。

a. 遺伝子変異の有無(DNAの変異)

癌細胞に高頻度に認めるDNA変異(点変異、欠失、増幅など)の有無を調べることで癌細胞の存在を検出する方法である。現在よく行われているものは、癌細胞に高頻度に認められる癌抑制遺伝子p53や癌遺伝子K-rasの変異(主に点突然変異)を検出する方法である。DNAの変異部位は様々であるため実際は高頻度にみられるhot spot部位の変異を検出している。p53では、コドン175, 245, 248, 249, 273, 282, K-rasではコドン12, 13, 61がhot spotである。遺伝子(DNA)変異の存在は癌細胞の存在を強く示唆するが、マクロファージなどに貪食されたviabilityのない癌細胞も検出してしまうことや、原発巣での変異の有無による症例の制約(p53でも50%前後)、同じ遺伝子の変異でも変異の場所が少なからず同じではないこと、遺伝子によってはその大きさなどから変異の検出が困難であることなどの問題がある。手技も煩雑である。ほかにも、遺伝子の欠失:LOH(ヘテロ接合性の消失)、マイクロサテライト不安定性など癌細胞に比較的特異的なDNA上の変化を検出する方法がある。

b. 遺伝子発現量の変化(mRNA, 蛋白量)

正常細胞と比較し癌細胞で変化する遺伝子の発現量を測定する方法である。MAGE(melanoma-associated antigen)などの癌精巣抗原は、癌細胞にほぼ特異的に発現するが、その発現癌細胞が少ないため単独では普遍性に乏しい。上皮細胞は、リンパ節、骨髄、末梢血には通常存在しないため、その存在は癌細胞を強く示唆する。CEAやサイトケラチン(CK)などの上皮特異的マーカーは、癌細胞に特異的ではないが上皮細胞のほぼすべてに発現し、発現量も多いため検

出が容易である。よって現在この上皮マーカーが微量癌細胞の検出マーカーとしてよく用いられており、特にmRNA量を測定するRT-PCR法では、CEA, CK8, CK18, CK19, CK20, mammaglobin(MMG), MUC1など、蛋白を検出する免疫染色法では、CEA, 各種CK, ECSAなどが頻用されている。CEAは臨床的にも腫瘍マーカーとして頻用されている腫瘍胎児性抗原である。CKは細胞骨格を形成する中間径線維の一つであり、その構成単位は少なくとも20種類以上ある。pseudogeneがあるためDNAの混入がある場合検出は困難となる。MMGは乳腺上皮に特異的に発現するといわれているが胆嚢上皮にも発現を認めるとの報告がある。MUC1は上皮性ムチン蛋白で、上皮性腫瘍の細胞膜に存在する。腫瘍マーカーとして頻用されているCA15-3はこのMUC1の抗体である。これらのマーカーを複数組み合わせることで検出感度を上げる試みもある。しかし、これらの上皮マーカーも微量ながらリンパ節、骨髄、末梢血に存在する単核球などの非上皮性細胞にも発現しているため、発現の有無を単純にall or none形式で表すことはできない。蛋白発現量検出法で一般的によく行われている方法は、抗原抗体反応を利用した免疫染色法である。標的マーカーの発現をその抗体で検出する。複数のCKを認識するAE1/AE3抗体(CK1-8, 10, 14-16, 19)や、CAM5.2抗体(CK8, 18, 19)などがよく用いられている。

c. 蛋白構造、機能の変化(例:酵素活性)

対象が限定されること、検出感度が非常に低いこと、解析が非常に煩雑なことなどの理由によりほとんど微量癌細胞の検出法としては用いられていない。

4. 微量癌細胞の検出法(表1)

微量癌細胞の検出法は、組織(細胞)染色法と分子生物学的手法の2つに大きく分類され、それぞれ利点、欠点がある。以下各々について概説する。

a. 組織(細胞)染色法

細胞、組織を染色し、形態学的に判断する方

表 1 微量癌細胞の代表的な検出法

方法	検出対象	標的マーカー	検出感度	特徴
免疫染色法	遺伝子発現の有無	蛋白レベル CEA, CK, etc	1/10 ⁴	簡便, 形態評価が可能 判定者の技量に依存
RT-PCR法	遺伝子発現量	mRNAレベル CEA, CK, etc	1/10 ⁶	客観的, 遺伝子発現の定量化, 最も好感度, viabilityのある細胞からのみ検出, 疑陽性
MASA法 etc	遺伝子変異の有無	DNAレベル p53, K-ras, etc	1/10 ⁴	癌細胞の直接存在証明, viabilityのない細胞も検出, 対象症例が限定

法である。免疫染色法では、形態に加えて抗原抗体反応により遺伝子発現の有無を高感度に検出できる。リンパ節の場合は、約5 μ mの厚さの薄切切片を数枚作製する。血液や骨髄の場合は、効率化のために、比重液を用いて細胞成分のみを分離し、スメア標本を作製する。簡便かつ試薬も比較的容易に入手できるためほとんどの施設で施行可能である。簡便であること、癌細胞であるかどうかを形態的に判断できることが利点である。しかし、問題点として、一つの検体に対しどれだけのスライド切片を作るべきか、判定者の技量など、検出率に大きくかわる検出上の問題に加え、検出した微量癌細胞のviabilityの有無の判定は不可能である。

1) H. E(ヘマトキシリン エオシン)染色法

一般の病理診断に用いられている染色法である。安価かつ最も簡便に短時間で診断可能な方法である。細胞や核の形態などにより癌細胞を判定する。しかしその判読にはかなりの熟練を要し、見逃す危険性が高い。

2) 免疫染色法

癌特異的マーカー(MAGEなど)や、リンパ節、血液、骨髄中に上皮系細胞が存在しないことを利用して上皮特異的マーカーを抗原抗体反応により検出する方法である。手技は簡便であり、H. E染色に比較し検出が容易(10⁴個の単核球に1個の癌細胞を検出)で、微量癌細胞の検出法として頻用されており、実際に免疫染色法を用いた微量癌細胞検出に関する報告が現在までのところ最も多く、この検出法が主流となっている。しかし、抗体が比較的高価であること、染色に時間を要すること、樹状細胞やマクロフ

ージなどの免疫担当細胞も陽性になるなどの疑陽性があり、判定困難な例が少なくないことなどの問題点がある。

b. 分子生物学的手法

細胞、組織からDNA, RNAを抽出して、遺伝子変異や遺伝子発現を分子生物学的手法を用いて検出することにより微量癌細胞の存在診断を行う方法である。近年のPCR法の開発により微量な遺伝子の増幅、解析が可能になった。ごくわずかな微量癌細胞も検出可能であること(10⁴-10⁶個の単核球中に1個の癌細胞を検出)、多数の細胞、組織を一塊として検査することができること、技術的にも比較的簡便であり客観的で再現性の高いこと、遺伝子発現量の定量化も可能であることが最大の利点である。しかし検査に専門的技術、器具、試薬を必要とする。

1) RT-PCR(reverse transcription-polymerize chain reaction)法

標的マーカーの遺伝子発現(mRNA)を検出する方法である。mRNAを直接検出する方法としてはNorthern blot法やRNA protection assayなどがあるが、検出感度がかなり低いこと、操作が煩雑なことなどにより通常用いられない。そこで、標的マーカーのmRNAを逆転写酵素を用いて逆転写反応(RT)させcDNAを作製し、それをPCR法で数百万倍に増幅することで生成されたPCR産物の量により判定するRT-PCR法が用いられている。検出感度は10⁵-10⁶個の単核球中に1個の癌細胞を検出できるほどで最も高い。ほぼすべての症例を対象にできること、mRNAはviableな癌細胞のみに発現することからその存在はviableな癌細胞の存在を意味する

こと、簡便かつ客観的で短時間で測定可能であること、標的マーカーも容易に変えられることなど多くの利点があるため、微小転移検出法として頻用されている。しかし、非常に微量な癌細胞を検出することができる一方、わずかな上皮細胞の混入も検出してしまうこと、CEAやCKなどの上皮マーカーも微量ながらリンパ節、骨髄、末梢血に存在する単核球などの非上皮性細胞にも発現していることから、従来のPCR産物をアガロースゲル電気泳動上でエチジウムブロマイド染色し、そのバンドの有無で遺伝子発現を判断する定性的方法では判定できない。発現の有無は相対的な発現量の差で判断する必要があるが、現在では従来のPCR法に変わって遺伝子発現量を正確に測定可能な定量的PCR法が主流になってきた。陰性コントロールを置き厳密にcut off値の設定を行う必要がある。RT-PCR法を行う際にはその検出度の高さから疑陽性の存在を念頭に置かねばならない。

2) DNA mutation (変異) の検出

癌細胞に高頻度に認めるDNA変異(点突然変異、欠失、増幅など)の有無を検出する方法である。よく用いられている方法は、点突然変異を検出する方法で、変異部位に特異的なプライマーを設定し変異を検出するMASA(mutant allele specific amplification)法や増幅されたDNAの構造的な多型を利用して変異を検出するPCR-SSCP(single strand conformational polymorphism)法、増幅したDNAの制限酵素の切断の有無で変異の検出を行うPCR-RFLP(restriction fragment length polymorphism)法などがある。検出感度は比較的感度の高いMASA法でも 10^4 個の単核球中に1個の癌細胞を検出できる程度である。検出感度を上げるためにMACS(magnetic-activated cell separation system; 磁気細胞分離システム: 細胞膜貫通型蛋白CD45が、癌細胞には認められず、単核球にのみ存在することを応用し、磁気ビーズを付着させたCD45抗体を用いて癌細胞と単核球とを分離する方法)⁹⁾を利用することもある。ほかに、定量的PCR法を用いたPCR産物の融解曲線解析により変異を検出する方法もある。

5. 乳癌における微小転移検出対象臓器

a. リンパ節

リンパ節転移の有無は乳癌の最大の予後因子である。リンパ節転移診断をより正確に診断することは進行度状況の把握と治療方針の決定に重要である。上記のように、通常の病理組織検査は、リンパ節全体の癌細胞を診断しているわけではないので、検出し得ない癌細胞の存在は十分に予想される。そこで、高感度な手法を用いてより正確に診断しようというものである。また、癌がリンパ流の方向から最初に転移すると考えられるセンチネルリンパ節の転移診断に応用することで従来の病理組織診断より精度が高く正確に転移診断を行えるとの報告があり^{7,8)}、更に術中に診断することでリンパ節郭清範囲を決定しようとする試みもある。

b. 血液

癌細胞の全身播種(血行性転移)の指標として用いられる。採取が簡便で低侵襲であるため、検診への応用、治療前後の治療効果の評価など様々な臨床応用が期待される。採取できる細胞数が少ないため、微量癌細胞検出には高感度なRT-PCR法などの分子生物学的手法が主として用いられている。

c. 骨髄

骨転移というより血液同様に癌細胞の全身播種の指標として用いられる。骨髄は癌転移のcommon homing organであり、また末梢血のフィルターとも考えられており^{9,10)}、末梢血よりも高感度に全身播種を検出できると予想されている。実際に現在までの報告をみると末梢血よりも骨髄における微量癌細胞の陽性率が高い。主として胸骨、腸骨、肋骨から採取する。採取部位や採取量により陽性率が異なるとの報告がある。

6. 微量癌細胞研究の新展開と癌転移機序の新たなモデル(図2)

近年single cell comparative genomic hybridization(CG)やDNAマイクロアレイなどが開発され1個の細胞の遺伝子変異解析が可能とな

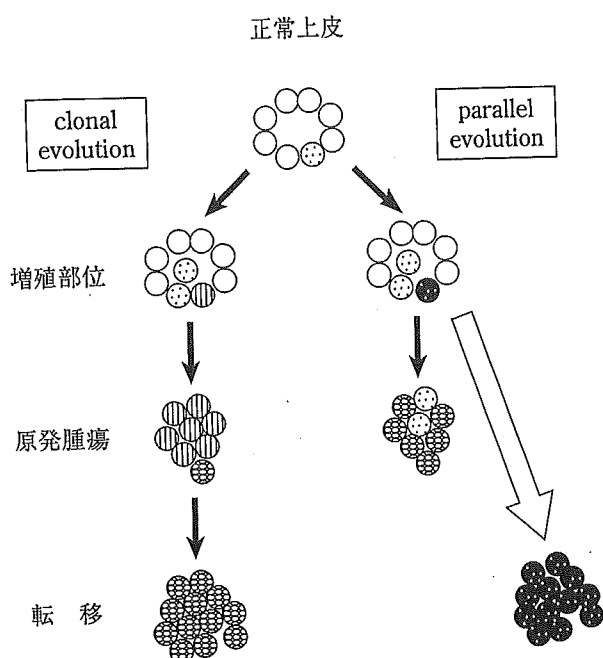


図2 癌転移の新たなモデル(文献¹³⁾より改変引用)
癌転移は極めて早期に生じ、原発巣とは別に増大していく(parallel evolution)。

り、微量癌細胞の遺伝子解析が行われるようになった。それにより興味深い知見が得られている。Kleinら¹¹⁾は、乳癌において骨髄、血液、リンパ節中のサイトケラチン陽性細胞(臨床的に転移陽性あるいは陰性(微量癌細胞))同士の遺伝子(染色体)変異をsingle cell CGHを用いて比較したところ、微量癌細胞おのおので異なっており、臨床的に転移陽性症例では遺伝子変異はかなり均一化していることを報告している。またSchmidt-Kittlerら¹²⁾は、乳癌において原発巣と骨髄中サイトケラチン陽性細胞(臨床的に転移陽性あるいは陰性(微量癌細胞))の遺伝子変異をsingle cell CGHを用いて比較すると、原発巣や転移巣に比較して微量癌細胞の遺伝子変異は有意に少なくかつランダムに認めるのに対し、原発巣や転移巣ではそれぞれ特徴的な遺伝子変異を認め、更にサイトケラチン陽性細胞の遺伝子変異パターンから臨床的に転移陽性症例と陰性症例とを分類することができることを報告している。これらの知見は、腫瘍細胞はかなり早い段階で原発巣より播種し、播種巣で転移細胞に特徴的な遺伝子変異を獲得していく可能性を示唆しており、以上から

Gray¹³⁾は、現在考えられている腫瘍の転移機序(clonal evolution: 原発巣で遺伝子変異を積み重ねて転移能を獲得する)とは異なるparallel evolutionを提唱している。

以上のように原発巣と播種巣の遺伝子変異が大きく異なるのであれば、現在行われている原発巣を対象にした治療法は播種巣には十分な効果が得られない可能性がある。また、微量癌細胞の多くは細胞周期G0期にありdormantな状態にあることが予想されるため、細胞周期依存性の化学療法は微量癌細胞には効果が期待できないと考えられる⁹⁾。実際に抗癌剤投与により骨髄中の微量癌細胞数は減少しないとの報告もある¹⁴⁾。したがって、原発巣だけでなく微小転移巣を対象とした治療法の選択、具体的には微小転移細胞の遺伝子解析に基づいた治療法選択が今後重要になってくると思われる。

7. 微小転移研究の現状と今後の展望

現在までの報告では、微小転移陽性率は、およそリンパ節15-30%、骨髄20-60%、末梢血20-30%程度の報告が多い¹⁵⁾。微小転移研究が始まって久しいが近年ようやく微小転移(骨髄・リンパ節)の臨床的意義が認識されつつあり、特に骨髄中の微小転移は新たな予後因子として認められつつある。しかし、信頼に足る大規模なstudyはまだ少なく、各施設で検出法、検出マーカーなどが異なっており、また、リンパ節、血液、骨髄いずれもBraunら¹⁶⁾の大規模studyの報告のように予後との関連ありとの報告が多いが関連なしとの報告¹⁵⁾も少なからずあることから依然臨床的意義が確立したとはいえない。欧米ではAmerican College of Surgeons Oncology Z0010 Trialなどの大規模studyが現在進行中である。著者らも、これまで微小転移の臨床的意義について検討を重ねてきたが¹⁷⁻²¹⁾、特に2000年からは九州がんセンター乳腺科との共同で1,000例を超える規模の骨髄、血液の微小転移研究プロジェクトを進行中である。

現在、微小転移検出法としてサイトケラチンを対象とした免疫染色法が主流となっているが上記のように様々な問題点がありそれらをどう

克服するのか、定量的 RT-PCR 法はルーチン検査となり得るのかなど、解決していくべき点は多い。しかし、微小転移の臨床的意義が確立すれば、Hawes らが提唱²²⁾するような TNn (リンパ節微小転移) Mm (骨髄微小転移) 分類などによる詳細な癌進行度分類が可能となり、患者一人一人に応じた治療 (テーラーメイド治療) が可能になると思われる。更に微小転移の遺伝子解析から、癌転移機序の解明ならびに、より効果的な癌治療法の開発が期待される。

おわりに

以上、乳癌における微小転移について概説した。まだ信頼に足る大規模 study は少ないが、微小転移の臨床的意義が認識されつつある現在、今後は微小転移の臨床的意義が検証されていくのと同時に、微小転移診断の臨床応用や微量癌細胞の基礎的研究に基づいた治療法の選択および開発に焦点があたっていくものと思われる。

■ 文 献

- 1) Solakoglu O, et al: Heterogeneous proliferative potential of occult metastatic cells in bone marrow of patients with solid epithelial tumors. *Proc Natl Acad Sci USA* 99: 2246-2251, 2002.
- 2) O'Sullivan GC, et al: Micrometastases in esophagogastric cancer: high detection rate in resected rib segments. *Gastroenterology* 116: 543-548, 1999.
- 3) Scheunemann P, et al: Tumorigenic potential of apparently tumor-free lymph nodes. *N Engl J Med* 340: 1687, 1999.
- 4) Heiss MM, et al: Individual development and uPA-receptor expression of disseminated tumor cells in bone marrow: a reference to early systemic disease in solid cancer. *Nat Med* 1: 1035-1039, 1995.
- 5) Braun S, et al: ErbB2 overexpression on occult metastatic cells in bone marrow predicts poor clinical outcome of stage I-III breast cancer patients. *Cancer Res* 61: 1890-1895, 2001.
- 6) Shibata K, et al: Detection of ras gene mutations in peripheral blood of carcinoma patients using CD45 immunomagnetic separation and nested mutant allele specific amplification. *Int J Oncol* 12: 1333-1338, 1998.
- 7) Kataoka A, et al: RT-PCR Detection of breast cancer cells in sentinel lymph nodes. *Int J Oncol* 16: 1147-1152, 2000.
- 8) Noguchi M: Therapeutic relevance of breast cancer micrometastases in sentinel lymph nodes. *Br J Surg* 89: 1505-1515, 2002.
- 9) Ozbas S, et al: Bone marrow micrometastasis in breast cancer. *Br J Surg* 90: 290-301, 2003.
- 10) Pantel K, Woelfle U: Micrometastasis in breast cancer and other solid tumors. *J Biol Regul Homeost Agents* 18: 120-125, 2004.
- 11) Klein CA, et al: Genetic heterogeneity of single disseminated tumour cells in minimal residual cancer. *Lancet* 360: 683-689, 2002.
- 12) Schmidt-Kittler O, et al: From latent disseminated cells to overt metastasis: genetic analysis of systemic breast cancer progression. *Proc Natl Acad Sci USA* 100: 7737-7742, 2003.
- 13) Gray JW: Evidence emerges for early metastasis and parallel evolution of primary and metastatic tumors. *Cancer Cell* 4: 4-6, 2003.
- 14) Braun S, et al: Lack of effect of adjuvant chemotherapy on the elimination of single dormant tumor cells in bone marrow of high-risk breast cancer patients. *J Clin Oncol* 18: 80-86, 2000.
- 15) Braun S, et al: Implications of occult metastatic cells for systemic cancer treatment in patients with breast or gastrointestinal cancer. *Surg Oncol* 20: 334-346, 2001.
- 16) Braun S, et al: Cytokeratin-positive cells in the bone marrow and survival of patients with stage I, II, or III breast cancer. *N Engl J Med* 342: 525-533, 2000.
- 17) Mori M, et al: Detection of cancer micrometastases in lymph nodes by reverse transcriptase-polymerase chain reaction. *Cancer Res* 55: 3417-3420, 1995.

- 18) Mori M, et al: Molecular detection of circulating solid carcinoma cells in the peripheral blood: the concept of early systemic disease. *Int J Cancer* 68: 739-743, 1996.
- 19) Mori M, et al: Clinical significance of molecular detection of carcinoma cells in lymph nodes and peripheral blood by reverse transcription-polymerase chain reaction in patients with gastrointestinal or breast carcinomas. *J Clin Oncol* 16: 128-132, 1998.
- 20) Etoh T, et al: Clinical significance of K-Ras mutation in intraoperative tumor drainage blood from patients with colorectal carcinoma. *Ann Surg Oncol* 8: 407-412, 2001.
- 21) Masuda TA, et al: Detection of occult cancer cells in peripheral blood and bone marrow by quantitative RT-PCR assay for cytokeratin-7 in breast cancer patients. *Int J Oncol* 26: 721-730, 2005.
- 22) Hawes D, et al: Detection of occult metastasis in patients with breast cancer. *Semin Surg Oncol* 20: 312-318, 2001.



A service of the National Library of Medicine
and the National Institutes of Health

My NCBI
[Sign In] [Register]

All Databases

PubMed

Nucleotide

Protein

Genome

Structure

OMIM

PMC

Journals

Books

Search PubMed for

Limits Preview/Index History Clipboard Details

About Entrez
NCBI Toolbar

Display Abstract Show 20 Sort by Send to

Text Version

All: 1 Review: 0

Entrez PubMed

1: [Int J Oncol.](#) 2006 Feb;28(2):297-306.

[Related Articles, Links](#)

Overview

Help | FAQ

Tutorials

New/Noteworthy

E-Utilities

Usefulness and clinical significance of quantitative real-time RT-PCR to detect isolated tumor cells in the peripheral blood and tumor drainage blood of patients with colorectal cancer.

PubMed Services

Journals Database

MeSH Database

Single Citation Matcher

Batch Citation Matcher

Clinical Queries

Special Queries

LinkOut

My NCBI

[Iinuma H](#), [Okinaga K](#), [Egami H](#), [Mimori K](#), [Hayashi N](#), [Nishida K](#), [Adachi M](#), [Mori M](#), [Sasako M](#).

Department of Surgery, Teikyo University School of Medicine, Itabashi-ku, Tokyo 173-0003, Japan. iinuma@med.teikyo-u.ac.jp

Related Resources

Order Documents

NLM Mobile

NLM Catalog

NLM Gateway

TOXNET

Consumer Health

Clinical Alerts

ClinicalTrials.gov

PubMed Central

The clinical significance of isolated tumor cells (ITC) circulating in the blood of patients with colorectal cancer is unclear. In this study, we investigated the relationship between the presence of ITC that express carcinoembryonic antigen (CEA) and/or cytokeratin 20 (CK20) transcripts in the blood and the clinicopathological findings and prognosis using the quantitative real-time reverse transcription-polymerase chain reaction (RT-PCR) assay. We studied peripheral blood and tumor drainage blood from 167 patients with colorectal cancer. Quantitative real-time RT-PCR assay was able to detect one tumor cell in 3×10^6 peripheral blood mononuclear cells. Applying a cut-off value, CEA and/or CK20 (CEA/CK20) were detected in 10.2% (17/167) of the patients' preoperative peripheral blood samples and 34.1% (57/167) of the patients' tumor drainage blood samples. In the relationship between the CEA/CK20 of the blood and the clinicopathological factors, a significant correlation was demonstrated between the positivity of marker genes and the depth of invasion, venous invasion, lymph node metastasis, liver metastasis or stage. The disease-free and overall survival of patients with CEA/CK20-positive peripheral or tumor drainage blood was significantly shorter than that of marker gene-negative patients. CEA/CK20 transcripts in tumor drainage blood were independent factors for prognosis in disease-free survival and overall survival. These results suggest that detecting CEA/CK20 mRNA in tumor drainage blood by real-time RT-PCR has prognostic value in patients with colorectal cancer. Large scale and long-term clinical studies are needed to confirm the prognostic value of genetically detecting ITC in the peripheral blood.

PMID: 16391782 [PubMed - in process]



A service of the National Library of Medicine
and the National Institutes of Health

My NCBI
[Sign In] [Registered]

All Databases PubMed Nucleotide Protein Genome Structure OMIM PMC Journals Books

Search PubMed for

Limits Preview/Index History Clipboard Details

About Entrez
NCBI Toolbar

Display Abstract Show 20 Sort by Send to

Text Version

All: 1 Review: 0

Entrez PubMed

1: [Stem Cells](#), 2006 Mar;24(3):506-13. Epub 2005 Oct 20.

[Related Articles](#), [Links](#)

Overview

Help | FAQ

Tutorials

New/Noteworthy

E-Utilities

Full text article at
stemcells.elsevier.com

Characterization of a side population of cancer cells from human gastrointestinal system.

[Haraguchi N](#), [Utsunomiya T](#), [Inoue H](#), [Tanaka F](#), [Mimori K](#), [Barnard GE](#), [Mori M](#).

Department of Surgery, Medical Institute of Bioregulation, Kyushu University, Tsurumihara 4546, Beppu 874-0838, Japan.
mmori@tsurumi.beppu.kyushu-u.ac.jp

PubMed Services

Journals Database

MeSH Database

Single Citation Matcher

Batch Citation Matcher

Clinical Queries

Special Queries

LinkOut

My NCBI

Related Resources

Order Documents

NLM Mobile

NLM Catalog

NLM Gateway

TOXNET

Consumer Health

Clinical Alerts

ClinicalTrials.gov

PubMed Central

A subset of stem cells, termed "side population" (SP) cells, has been identified and characterized in several mammalian tissues and cell lines. However, SP cells have never been identified or isolated from gastrointestinal cancers. We used flow cytometry and the DNA-binding dye Hoechst 33342 to isolate SP cells from various human gastrointestinal system cancer cell lines. Fifteen of sixteen cancer cell lines from the gastrointestinal system contained 0.3%-2.2% SP cells. Next, we used an oligonucleotide microarray to analyze differentially expressed genes between SP and non-SP cells of hepatoma HuH7. The expression of GATA6, which is associated with embryonic development and hepatocytic differentiation, was significantly upregulated in HuH7 SP cells. The expression of ABCG2, ABCB1, and CEACAM6, which are associated with chemoresistance, was also significantly increased in SP cells. In addition, some epithelial markers and mesenchymal markers were overexpressed in SP cells. Reverse transcription-polymerase chain reaction and immunocytochemical staining validated these results and suggested a multilineage potential for HuH7 SP cells. In hepatoma HuH7 and colorectal SW480 cell lines, SP cells showed evidence for self-renewal, generating both SP and non-SP cells. Finally, chemoresistance to anticancer agents, including doxorubicin, 5-fluorouracil, and gemcitabine, were compared between HuH7 SP and non-SP cells using an ATP bioluminescence assay. The HuH7 SP cells expressed a higher resistance to doxorubicin, 5-fluorouracil, and gemcitabine compared with non-SP cells. These findings demonstrate that cancers of the gastrointestinal system do contain SP cells that show some characteristics of so-called stem cells.

PMID: 16239320 [PubMed - in process]

PGP9.5 Methylation in Diffuse-Type Gastric Cancer

Keishi Yamashita,¹ Hannah Lui Park,¹ Myoung Sook Kim,¹ Motonobu Osada,¹ Yutaka Tokumaru,¹ Hiroshi Inoue,² Masaki Mori,² and David Sidransky¹

¹Department of Otolaryngology, Division of Head and Neck Cancer Research, Johns Hopkins University, Baltimore, Maryland and

²Department of Surgical Oncology, Medical Institute of Bioregulation, Kyushu University, Tsurumibarū, Beppu, Japan

Abstract

Diffuse-type gastric cancer (DGC) is the most deadly form of gastric cancer and is frequently accompanied by peritoneal dissemination and metastasis. The specific molecular events involved in DGC pathogenesis remain elusive. Accumulating evidence of epigenetic inactivation in tumor suppressor genes led us to conduct a comprehensive screen to identify novel methylated genes in human cancers using pharmacologic unmasking and subsequent microarray analysis. We compared differential RNA expression profiles of DGC and intestinal-type gastric cancer (IGC) cell lines treated with 5-aza-2'-deoxycytidine using microarrays containing 22,284 genes. We identified 16 methylated genes, including many novel genes, in DGC cell lines and studied *PGP9.5* with particular interest. In primary gastric cancers, *PGP9.5* was found to be more frequently methylated in DGCs (78%) than in IGCs (36%; DGC versus IGC, $P < 0.05$). Furthermore, real-time methylation-specific PCR analysis of *PGP9.5* showed relatively higher methylation levels in DGC than in IGC. Our data thus implicate a molecular event common in the DGC phenotype compared with IGC. (Cancer Res 2006; 66(7): 3921-7)

Introduction

Uncontrollable tumor invasion and dissemination of cancer cells around the primary organ is the neoplastic process responsible for most deaths from cancer due to inadequacy of surgical removal (1). Invasive and metastatic cancer cells have undergone numerous genetic and epigenetic changes, manifested by cytoskeletal changes, loss of adhesion, and expression of proteolytic enzymes that degrade the basement membrane (2). Among gastric cancers, diffuse-type gastric cancers (DGC) exhibit a higher frequency of invasion with dissemination to the peritoneum and lymph node metastasis compared with intestinal gastric carcinomas (IGC; refs. 3, 4). In addition, signet ring cells, which are found in DGC, show marked morphologic and phenotypic alterations from non-signet ring gastric cancer cells, such as anchorage-independent growth, resistance to cellular adhesion, and resistance to apoptosis

(5–8). Much remains to be learned about the transition from normal gastric epithelial cells to cells capable of invading surrounding tissues and metastasis. Moreover, further progress in the treatment or prevention of DGC is contingent upon identifying novel genes and pathways that are consistently and specifically altered in disseminated cells.

Differences in the clinicopathologic features between IGC and DGC have led investigators to believe that two distinct pathways are involved in their pathogenesis. Using Lauren's approach to histologic classification (DGC versus IGC), the average age of onset for DGC was reported to be 56 years, 10 years earlier than for IGC (4, 9, 10), and there was a significantly higher percentage of DGC without associated (atrophic) gastritis, a presumed causal lesion of IGC (9). The rate of IGC is more than double in men than in women; however, there is no difference in the rate of DGC between the sexes (4, 10, 11). Genetic predisposition to gastric cancer is also more commonly associated with DGC than IGC (4, 12).

E-cadherin is somatically mutated in ~50% of sporadic DGC cases but not in IGCs (13), and germ line mutations have been found in familial DGCs (14). Interestingly, the second hit in *E-cadherin* germ line mutation carriers is generally due to methylation (15, 16). Furthermore, *E-cadherin* was recently found to be methylated more frequently in sporadic DGCs; 80% of DGC cases harbored methylation, whereas IGCs displayed methylation in only 30% of cases (17). However, *E-cadherin* is still inactivated in a substantial number of IGC tumors and other cancers with completely different morphologies (17, 18); thus, inactivation of *E-cadherin* is unlikely to be the exclusive determinant of the DGC-specific phenotype.

Recently, hypermethylation of gene promoters has been explored as both a mechanism and marker of carcinoma progression (19–22). We have had great success in identifying novel cancer-specific methylated genes by pharmacologic unmasking [5-aza-2'-deoxycytidine (5Aza-dC) treatment] and subsequent microarray (PUM) analysis for esophageal and head and neck squamous cell carcinomas (HNSCC; refs. 23, 24). In this study, we applied this novel approach, using differential PUM between DGC and IGC, to identify novel methylated genes more specifically involved in the formation of DGC.

Materials and Methods

Cell lines and tissue samples. The following gastric cancer cell lines were used: NUGC3 (undifferentiated DGC), NUGC4 (signet ring cell DGC), KATOIII (signet ring cell DGC), AZ521 (highly differentiated IGC), and MKN7 (highly differentiated IGC). These cell lines were obtained from the Cell Response Center for Biomedical Research Institute in the Department of Aging and Cancer, Tohoku University. Cell lines were grown in RPMI 1640 supplemented with 10% fetal bovine serum for isolation of DNA and RNA.

Thirty-one pairs of primary gastric cancers and their corresponding adjacent normal tissue specimens were obtained from patients who had

Note: Supplementary data for this article are available at Cancer Research Online (<http://cancerres.aacrjournals.org/>).

K. Yamashita and H.L. Park equally contributed to this work.

Under a licensing agreement between Oncomethylome Sciences, SA and the Johns Hopkins University, D. Sidransky is entitled to a share of royalty received by the University upon sales of products described in this article. He owns Oncomethylome Sciences, SA stock, which is subject to certain restrictions under University policy. He is a paid consultant to Oncomethylome Sciences, SA and is a paid member of the company's Scientific Advisory Board. The Johns Hopkins University in accordance with its conflict of interest policies is managing the terms of this agreement.

Requests for reprints: David Sidransky, Department of Otolaryngology, Division of Head and Neck Cancer Research, Johns Hopkins University, 818 Ross Building, 720 Rutland Avenue, Baltimore, MD 21205-2196. Phone: 410-502-5152; Fax: 410-614-1411; E-mail: dsidrans@jhmi.edu.

©2006 American Association for Cancer Research.
doi:10.1158/0008-5472.CAN-05-1511

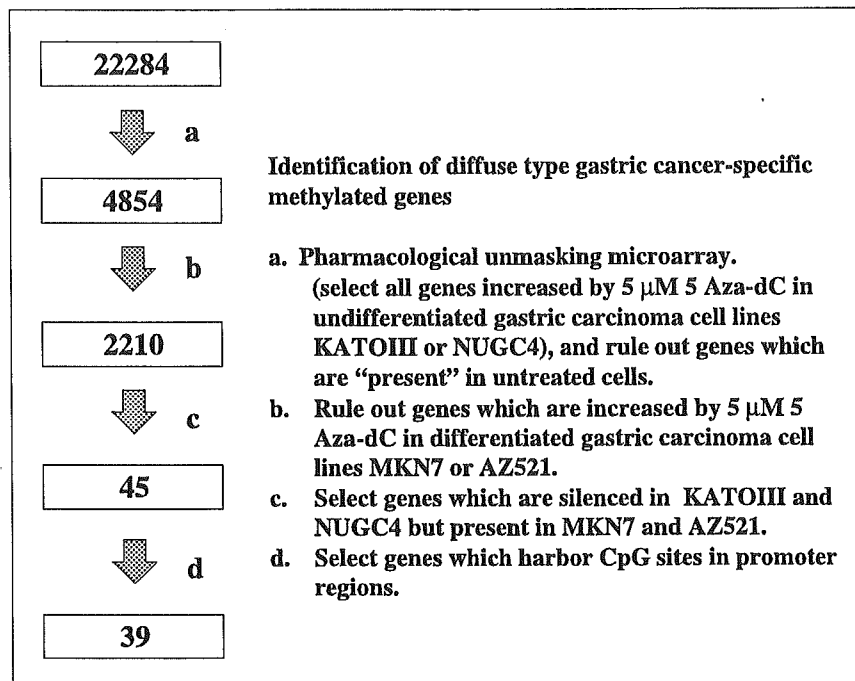


Figure 1. Flowchart for selection of candidate tumor suppressor genes. To screen for candidate markers specific to DGC, we treated four gastric cancer cell lines with 5 μmol/L 5Aza-dC and did microarray analysis using microarrays containing 22,284 genes. We obtained 4,854 candidates that showed absence of expression in any untreated DGC cell line and an increase in expression after treatment. We diminished the number of candidates by ruling out genes also increased in IGC cell lines, and 2,210 genes remained. We further reduced the number of candidate genes by only choosing genes with restricted expression profiles (see text), and 45 genes remained. We finally selected 39 genes that contained CpG islands to examine for methylation analysis.

undergone surgery in the Department of Surgical Oncology at the Medical Institute of Bioregulation, Kyushu University and the Department of Surgery at Oita Prefectural Hospital. The 40 cases were composed of 18 DGCs and 22 IGCs. Specimens were obtained from tumors, avoiding necrotic centers, immediately after resection. Corresponding normal mucosa specimens, which were at least 5 cm away from the tumor edge, were also obtained by sharply dissecting the mucosa off the muscularis propria. All specimens were quick frozen in liquid nitrogen and stored at -80°C until processing.

Pharmacologic unmasking (5Aza-dC treatment) of gastric cancer cells. Cells were split to low density (1×10^6 per T-75 flask) 12 to 24 hours before treatment. Cells were then treated for 4 days with 5 μmol/L 5Aza-dC (Sigma, St. Louis, MO) dissolved in 50% acetic acid/PBS or were mock treated with the same amount of acetic acid/PBS as done previously (23).

Microarray and reverse transcription-PCR analysis. We did oligonucleotide microarray analysis on the GeneChip Human Genome U133A Array (Affymetrix, Santa Clara, CA) containing 22,284 genes as per the

Table 1. Promoter methylation in DGC cell lines

Gene no.	Gene name	CpG*	Chromosomal	NUGC3	KATOIII	NUGC4	AZ521	MKN7	Methods
1	NM_004181 <i>PGP9.5</i>	(+)	4p14	M	M	M	U	U	SQ
2	AL136939 <i>Homologue of yeast LCEAE</i>	(+)	6p21	U	M	M	M	M/U	SQ
3	NM_024576 <i>FLJ21079 (Opioid receptor-like)</i>	(+?)	6q13	M	M	U	U	U	SQ
4	M60485 <i>Fibroblast growth factor receptor (FGFR)</i>	(+)	8p11	U	M	M/U	M/U	U	MSP
5	NM_023929 <i>Zinc finger protein RINZF</i>	(+)	8q13-21	U	M	U	U	U	SQ
6	U38945 <i>p16</i>	(+)	9p22	M	M	D	M	U	SQ
7	NM_000170 <i>Glycine dehydrogenase</i>	(+)	9p22	D	M	M	U	U	SQ
8	NM_014368 <i>LIM-6</i>	(+)	9q34	M/U	M	U	U	U	MSP
9	AL157398 <i>Nebulette</i>	(+)	10p12	M/U	M	U	U	U	MSP
10	NM_002906 <i>Radixin</i>	(+?)	11q23	U	M	U	U	U	SQ
11	NM_014333 <i>TLSC1</i>	(+)	11q23	U	M	M	U	M/U	SQ
12	NM_006931 <i>GLUT3 (SLC14)</i>	(+)	12p13	M	M	M	M	M	SQ
13	NM_025083 <i>FLJ21128</i>	(+)	15q23-24	U	M	U	U	U	SQ
14	AI358867 <i>Apolipoprotein E</i>	(+)	19q13	D	M	M	D	U	SQ
15	NM_003098 <i>Syntrophin α 1</i>	(+)	20q11	D	M	D	U	U	SQ
16	NM_014258 <i>Synaptonemal complex protein 2</i>	(+?)	20q13	M	M	M	M	M	SQ

Abbreviations: M, methylated; U, unmethylated; D, homozygous deletion or difficult to amplify DNA; SQ, sequencing after bisulfite treatment; MSP, methylation specific PCR.

*(+), dense CpG close to transcription start site; (+?), dense CpG island far from transcription start site (>2 kb).

manufacturer's instruction and identified genes up-regulated by pharmacologic treatment according to the manufacturer's algorithm. We isolated total RNA using Qiazol (Invitrogen, Carlsbad, CA), reverse-transcribed total RNA (8 µg) with Moloney murine leukemia virus (Invitrogen), and used one hundredth of the cDNA as a template for PCR. Reverse transcription-PCR (RT-PCR) was done for 24 to 30 cycles of 95°C for 1 minute, 54°C or 56°C for 1 minute, and 72°C for 1 minute or by touch-down PCR, depending on the gene. Primer sequences are available on request.

Bisulfite treatment of DNA. We extracted genomic DNA from Qiazol-treated samples and did bisulfite modification of genomic DNA as described (23). For DNA denaturing, 2 µg of genomic DNA were incubated with 5 µg salmon sperm DNA (Sigma) in 0.3 mol/L NaOH for 20 minutes at 50°C. The DNA sample was then diluted with 500 µL of a 2.5 mol/L sodium metabisulfite/125 mmol/L hydroquinone/0.4 mol/L sodium hydroxide solution and placed at 70°C for 1 hour. The sample was then applied to a column (Wizard DNA Clean Up System, Promega, Inc., Madison, WI), incubated with 0.3 mol/L NaOH for 10 minutes, and treated with 3 mol/L ammonium acetate for 5 minutes; 2.5-fold volume of 100% ethanol was added, and DNA was allowed to precipitate for 1 hour at room temperature. DNA was resuspended in 100 µL LoTE composed of 10 µmol/L Tris-HCl, pH 8 (Quality Biological, Inc., Gaithersburg, MD) and 2.5 µmol/L EDTA, pH 8 (Invitrogen) and stored at -80°C.

PCR amplification of bisulfite-treated DNA for sequencing. The primers were designed to recognize DNA alterations caused by the bisulfite treatment. Oligonucleotide primer pairs were purchased from Invitrogen. PCR amplifications were done as follows: a 5-minute 95°C incubation step followed by 45 cycles of 1 minute at 95°C, 1 minute at 54°C, and 2 minutes at 72°C. A 7-minute elongation step at 72°C completed the PCR amplification program. Primer sequences are listed in Supplementary Table S1.

Methylation-specific PCR. Bisulfite-treated DNA was amplified with either a methylation-specific or unmethylated-specific primer set for LIM homeobox protein 6 (*LIM-6*), *FGFR*, and *Nebulette*. The primers for methylated *LIM-6* were 5'-ACGACGAAACCGACGCTCG-3' and 5'-GGCGGGGTCGTTTTCGGTCG-3'. The primers specific for unmethylated *LIM-6* were 5'-CCAAAACAACAAAACCAACCTCA-3' and 5'-TTGGTGG-TGGGGTTGTTTTTGGTTG-3'. The primers specific for methylated *FGFR* were 5'-GACGCATAACGCTCGAAACG-3' and 5'-TAGCGGCGCG-TTCGCGGTCG-3'. The primers specific for unmethylated *FGFR* were 5'-CCACCAACACATAACACTCAAACA-3' and 5'-TTAAGTAGTGGTGT-GTTTGGTTG-3'. The primers specific for methylated *Nebulette* were 5'-CGCGAACGAAAACGCCAACG-3' and 5'-GGAGGGGGCGCGGTTTCGTCG-3'. The primers specific for unmethylated *Nebulette* were 5'-AAACACA-CAAACAAAACACCAACA-3' and 5'-GGAGGGGGTGTGGTTTGTG-3'. PCR reactions were done for 35 cycles of 95°C for 30 seconds, 59°C to 61°C for 30 seconds, and 72°C for 30 seconds.

Real-time quantitative methylation-specific PCR of bisulfite-treated DNA. For Taqman methylation-specific PCR (MSP), fluorescent probe and primer sets were designed to hybridize to the amplified region of DNA (25). The β -actin primer sequences were used as an internal control and previously described (24). For all reactions, 3 µL of bisulfite-treated DNA were added to a final volume of 20 µL. Serial dilutions of *in vitro* methylated human leukocyte DNA were used to construct a calibration curve, and all reactions were done in duplicate. The methylation ratio was defined as quantity of fluorescence intensity derived from *PGP9.5* promoter amplification divided by fluorescence intensity from β -actin amplification, multiplied by 100 (we designated this value as the Taqman methylation value: TaqMeth V).

Results

Differential PUM analysis between DGC and IGC cell lines.

We did a comprehensive survey for DGC-specific tumor suppressor gene candidates by comparing mock-treated and 5Aza-dC-treated gastric cancer cells. Our analysis included four cell lines, two derived from DGCs (NUGC4 and KATOIII, both signet ring cell

carcinomas) and two derived from IGCs (AZ521 and MKN7, both highly differentiated adenocarcinomas). We previously found that 5 µmol/L 5Aza-dC treatment resulted in reexpression of >85% of silenced transcripts also identified by more complex treatments, including either a lower dose of 5Aza-dC alone or in combination with trichostatin A (23). Thus, after treatment with 5 µmol/L 5Aza-dC for 4 days, isolated cell line RNA was hybridized to Affymetrix microarrays containing 22,284 transcripts. This procedure was nearly identical to that used in our previous studies, but the arrays used in our present study include more genes than previously contained in our esophageal squamous cell carcinoma (ESCC; ref. 23) and HNSCC (24) studies.

Complete silencing of expression is characteristic of methylated genes (23, 24); we, therefore, removed genes showing "present" expression in all four cell lines before pharmacologic treatment. After ruling out such genes, 4,854 unique genes remained, which were significantly up-regulated in at least one of the two DGC cell lines treated with 5 µmol/L 5Aza-dC compared with mock-treated cells (Fig. 1). To produce a more DGC-specific gene list, we further ruled out genes increased after pharmacologic unmasking of IGC cell lines, and 2,210 genes remained. We finally selected 45 genes that exhibited a profile of complete absence in the DGC cell lines and expression in the IGC cell lines, because putative DGC-specific tumor suppressor genes are likely to be more relevant if they are completely silenced in DGCs. Among the 45 remaining genes, 38 genes (84.4%) harbored CpG islands in their promoters by visual examination.

Identification of genes more frequently methylated in DGC cell lines. From the 38 genes examined for promoter DNA methylation, we identified 16 methylated genes in gastric cancer cell lines by using bisulfite DNA sequencing or MSP (Table 1). For methylation analysis, we added one more DGC cell line (NUGC3), which is not a signet ring cell carcinoma but an undifferentiated adenocarcinoma. Representative methylation is shown in Fig. 2A and B. Among the 16 genes, the methylation status of 14 genes was generally consistent with their gene expression profile in microarray (Table 1). The remaining two genes were *GLUT3* (*SLC14*) and *Synaptonemal complex protein 2*, both of which were methylated in all five gastric cancer cell lines tested (Fig. 2B).

PGP9.5 was the only gene specifically methylated in all three DGC cell lines but not in the two IGC cell lines (Table 1). Nine genes were also found to be methylated specifically in DGC cell lines, including *FLJ21079* (*Opioid receptor-like*), *Zinc finger protein RINZE*, *Glycine dehydrogenase*, *LIM-6*, *Nebulette*, *Radixin*, *FLJ21128*, *Apolipoprotein E*, and *Syntrophin α 1* (Fig. 2A and C; Table 1). Thus, these 10 genes showed DGC-specific methylation in our cell line analysis. The remaining four genes (*Homologue of yeast LCEAE*, *FGFR*, *p16*, and *TSLC1*) were not specifically methylated in DGC cell lines but may still be involved in DGC pathogenesis. By RT-PCR, these latter genes were silenced in expression in DGC, reactivated by pharmacologic unmasking, and present in IGC before treatment (Fig. 3).

***PGP9.5* is more frequently methylated in DGC cell lines and primary DGC tumors.** Among these genes, *PGP9.5* and *TSLC1* were of particular interest because *PGP9.5* was the only gene methylated specifically in all the DGC cell lines tested, and *TSLC1* was the only gene that was completely silenced in signet ring cell carcinoma cell lines (NUGC4 and KATOIII) yet expressed in both IGC cell lines (Fig. 3). Previous analyses have revealed that methylation patterns of many genes in primary cancer tissues are not necessarily consistent with those in cancer cell lines; thus, we examined the methylation

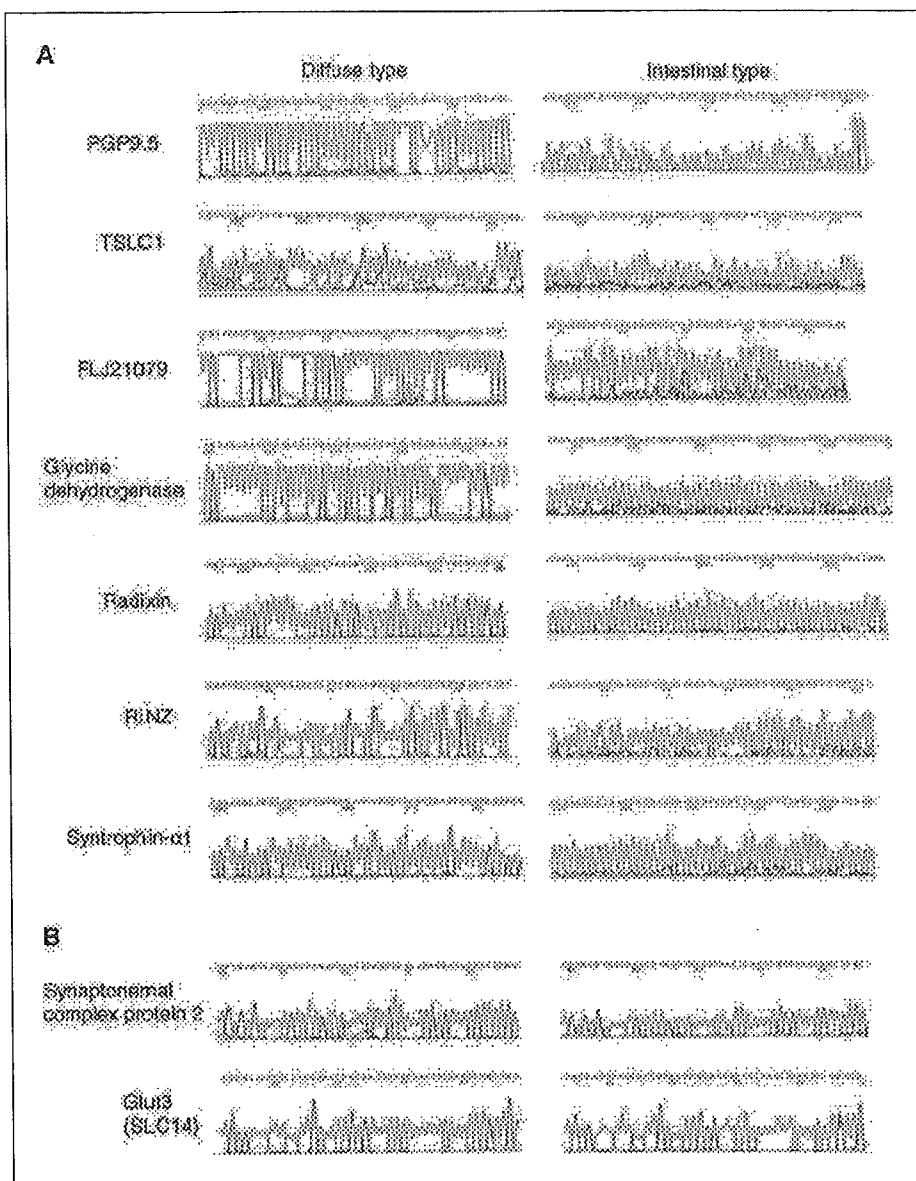


Figure 2. Promoter methylation analysis of several candidate markers specific to DGC. *A*, representative examples of direct sequencing analysis of bisulfite-treated DNA from DGC and IGC cell lines. *PGP9.5* (NUGC3 and AZ521), *TSLC1* (KATOIII and MKN7), *FLJ21079* (NUGC3 and MKN7), *Glycine dehydrogenase* (KATOIII and MKN7), *Radixin* (KATOIII and MKN7), *RINZ* (KATOIII and MKN7), and *Synaptrophin alpha 1* (KATOIII and MKN7) in DGC (*left*) and IGC (*right*). All guanines (*black peaks*) present after sequencing are derived from methyl cytosines on the complementary strand. *B*, methylation of two genes was not specific to DGC cell lines.

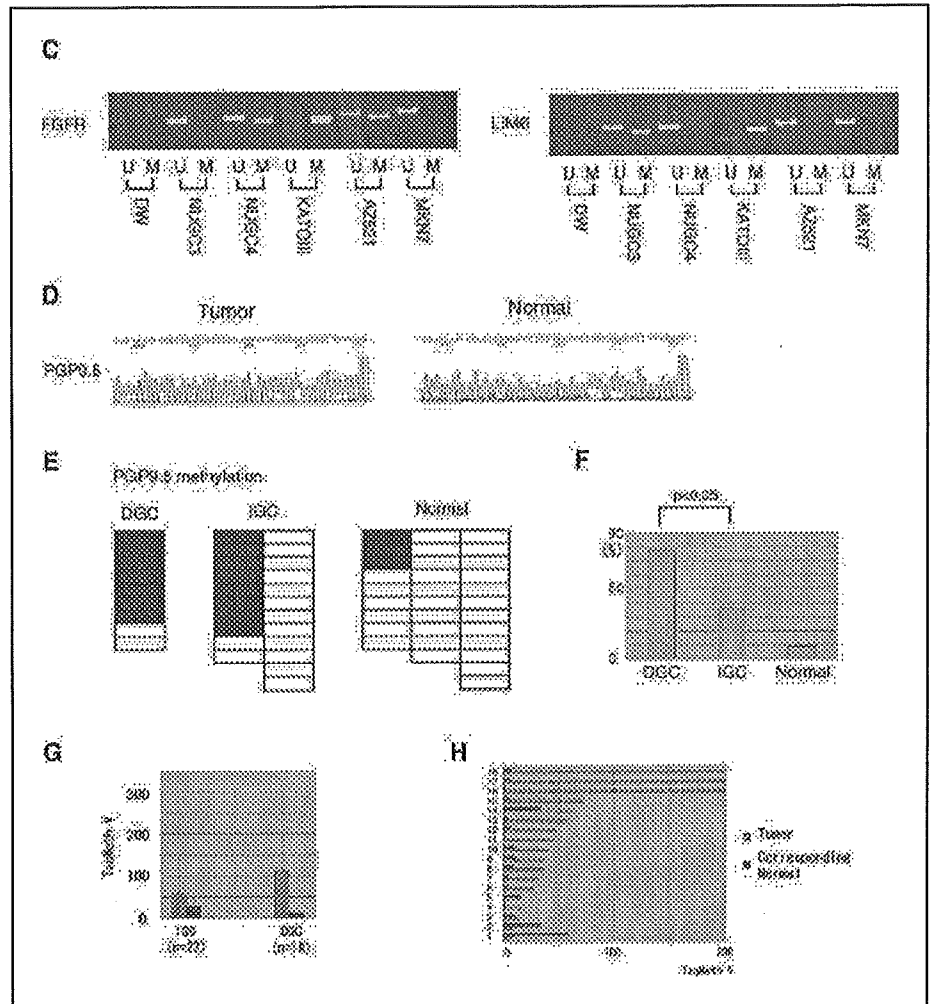
status of *PGP9.5* and *TSLC1* by direct sequencing after bisulfite treatment in primary gastric cancer tissue specimens comprised of DGCs ($n = 9$) and IGCs ($n = 22$), as well as their corresponding normal gastric epithelium ($n = 31$). For *PGP9.5*, there was little methylation in the adjacent normal epithelium from these cases (3 of 31 cases, 9.7%), some methylation in IGC specimens (8 of 22 cases, 36.4%), and significantly more frequent methylation in DGC (7 of 9 cases, 77.8%; IGC versus DGC, $P < 0.05$; Fig. 2*E* and *F*). Representative results of *PGP9.5* bisulfite sequencing for primary cancer and normal adjacent tissues are shown in Fig. 2*D*. By quantitative analysis using real-time MSP, *PGP9.5* methylation levels were higher in DGCs ($n = 18$) than in IGCs ($n = 22$; Fig. 2*G*). On the other hand, *TSLC1* methylation did not show any specificity in primary DGC tissue specimens (23.8% versus 20% in DGCs versus IGCs, respectively), consistent with our cell line data and the previously published data in gastric cancers (26).

Discussion

At the time of diagnosis, DGCs generally exhibit features of a more advanced stage, including more frequent peritoneal dissemination, lymph node metastasis, and nerve permeation, than IGCs (3, 4). Clinical studies have shown that DGCs have significantly worse prognosis than IGCs when considering the same pT (pT₃), sex (male), and age group. Moreover, a worse prognosis for DGC is influenced more by the incidence of regional lymph node involvement than by any other factors (27, 28). Although no difference in incidences of proximal gastric adenocarcinoma and distal adenocarcinoma has been seen, residual tumor was more frequently associated with DGCs ($P < 0.01$; ref. 29). These data suggest the existence of different pathogenic processes for these two histologic subtypes of gastric cancers.

No differences in classic tumor markers, such as carcinoembryonic antigen and α -fetoprotein, were found between DGC and

Figure 2. *Continued.* **C**, for genes that could not be analyzed by direct sequencing, we did conventional MSP to determine methylation status. MSP results for *FGFR* and *LIM-5* in five gastric cancer cell lines. *DW*, distilled water. **D**, *PGP9.5* methylation in primary DGC and corresponding normal mucosa tissue specimens. This region is the same as that examined in the cell lines shown in (**A**). **E**, methylation analysis for *PGP9.5* and *TSLC1* in primary gastric tumors and corresponding adjacent normal tissue. Green boxes indicate methylation of the promoter region. Nine DGCs, 22 IGCs, and 31 corresponding adjacent normal tissue specimens were examined. **F**, *PGP9.5* methylation is more commonly found in DGC (78%) than in IGC tissues (38%, $P < 0.05$). **G**, quantitative evaluation of *PGP9.5* methylation levels showed that *PGP9.5* methylation (TaqMeth V) was higher in DGCs ($n = 18$) than in IGCs ($n = 22$). Methylation levels of the corresponding adjacent normal tissues (black bars). **H**, DGC tissues showed higher hypermethylation levels of the *PGP9.5* promoter region compared to the corresponding normal tissues by quantitative real-time MSP analysis.



IGC (30). On the other hand, there have been reports on a number of genes that exhibit differential expression in DGCs and IGCs, such as M1, a mucin antigen (31); HLA-DR antigen (32); p53 protein accumulation (33, 34); and insulin-like growth factor-2 (35). Epigenetic events are one of the most upstream alterations, which could result in changes in expression of multiple genes, and there have been few reports of epigenetic differences between DGC and IGC, such as *E-cadherin* (17). In the current study, we found that *PGP9.5* exhibits more frequent methylation in DGCs than in IGCs and thus may be involved in DGC pathogenesis.

Less frequent methylation of *PGP9.5* was also found in the corresponding normal tissue (9.7%) as well as in IGC tumors (36.4%). Detection of *PGP9.5* methylation in matched adjacent normal-appearing tissue likely reflects surrounding field effects in patients with cancer. Normal tissue from patients without cancer remains to be tested in gastric cancer but is likely to be free of *PGP9.5* methylation (24). The level of specificity of *PGP9.5* methylation in primary DGC is similar to that of *E-cadherin*, which is also more frequently methylated in DGC, but not strictly specific (80% and 30%; ref. 17). Methylation of *E-cadherin* is also sometimes present in normal-appearing mucosa (18), whereas *E-cadherin* mutation is only seen in cancer (50% in DGC and absent in both IGC and normal tissues; ref. 13).

PGP9.5 has recently been reported as an onco-related molecule and potential tumor suppressor gene. *PGP9.5* was identified as a cancer-specific methylated gene in pancreatic cancer (36) and HNSCC by using PUM (24). In pancreatic cancer, *PGP9.5* was found to be methylated in almost all the cases (100%). Recently, we also profiled the methylation status of *PGP9.5* in ESCCs by real-time MSP and determined that its methylation was clearly associated with worse prognosis in ESCC ($P = 0.01$; ref. 25). Thus, *PGP9.5* may serve as a biomarker of more aggressive disease. We recently obtained functional evidence that *PGP9.5* inhibits log phase cell growth in culture and anchorage-independent growth and promotes apoptosis.³ Hence, there is increasing evidence that *PGP9.5* is both a tumor suppressor gene and a useful biomarker for certain cancers.

Promoter methylation of six genes (*FGFR*, *TSLC1*, *GLUT3*, *Synaptonemal complex protein 2*, *Homologue of yeast LCF4E*, and *p16*) was not specifically methylated in DGC cell lines. Some of these genes could represent artifacts of the screening process in which differences in expression are exaggerated due to technical issues. Two genes [*GLUT3* (*SLC14*) and *Synaptonemal complex*

³ In preparation.

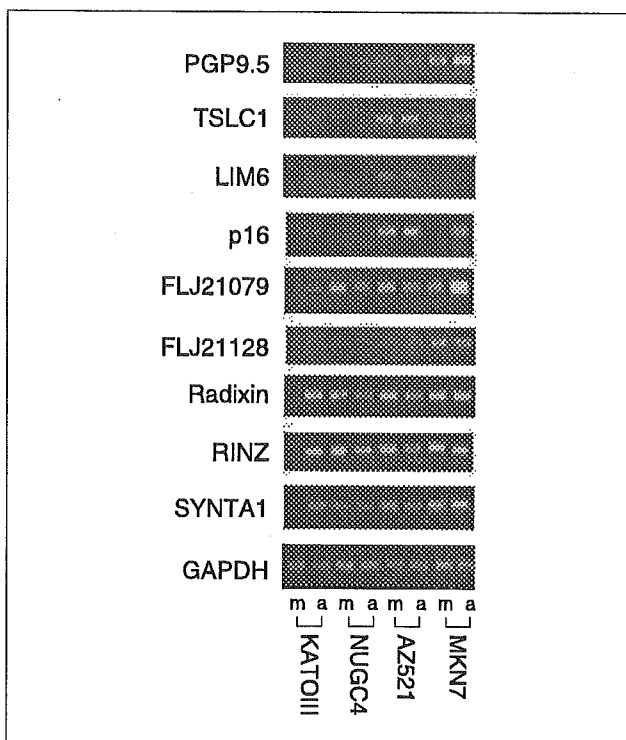


Figure 3. Pharmacologically reactivated genes identified by microarray and selected by the algorithm outlined in Fig. 1. These genes are candidates for specific silencing in DGC. *GAPDH* expression was used to confirm equal loading in each lane. *m*, mock; acetic acid/PBS; *a*, 5Aza-dC in the same volume of acetic acid/PBS.

protein 2] were methylated in all five gastric cancer cell lines tested (Fig. 2B), suggesting that the promoter regions we selected for investigating methylation are not critical for regulating gene expression. *AP-2* α and *trypsinogen* are such examples in which methylation of precise regions of promoter DNA correlates with gene expression status despite ubiquitous methylation of adjacent promoter regions (37, 38). In these cases, further analysis through the whole promoter region is needed to identify the exact region involved in regulating gene expression.

Surprisingly, *TSLC1* was not robustly reactivated in both DGC cell lines (slight reactivation in KATO III). This suggests differential sensitivity of the *TSLC1* promoter to demethylating agents or that other events (not necessarily epigenetic events) may also be involved in silencing *TSLC1* expression. In the DGC cell line KATO III, E-cadherin was previously found to be abrogated by gene mutation (39); it is possible that *TSLC1* expression may be influenced by the E-cadherin pathway. On the other hand, for the

other two genes (*p16* and *Homologue of yeast LCF1E*), we observed complete methylation of promoter CpG islands but abundant expression in AZ521 cells. This lack of correlation indicates that methylation is not always sufficient to cause gene silencing in cancer. For example, histone acetylation is an alternate mechanism that regulates gene expression, and synergistic suppression is well known to be required for complete silencing of several tumor suppressor genes (40). Our observation that *p16* is up-regulated by 5Aza-dC but is unmethylated in MKN7 cells suggests that *p16* may also, in some cases, be a downstream target of a methylated gene that is reactivated with treatment.

Further experiments will be required to definitively determine the molecular mechanisms through which *PGP9.5* affects the phenotype of DGC, but one of the most important ramifications of our current observation concerns its diagnostic potential. MSP after candidate gene identification allows timely and robust analysis of primary tumors and constitutes a promising molecular detection approach (18, 41–46). *PGP9.5* methylation is not strictly specific to DGCs; we observed that IGCs and corresponding normal tissues also harbored methylation but at a less frequent rate than in DGCs. In addition, background methylation in the corresponding normal tissues was lower in DGCs than in IGCs, which resulted in a more remarkable contrast between DGC cancer tissues and their corresponding normal tissues compared with IGCs (Fig. 2G). This difference in background methylation may be due to the difference in age distribution between patients with DGC and IGC. With its high sensitivity and specificity in primary DGC, *PGP9.5* methylation has potential to be developed as a biomarker to detect DGC in bodily fluids.

Finally, we showed in this study that differential PUM is a powerful tool to identify specific disease-related methylation events. This strategy enabled us to identify *PGP9.5* as a gene that is more frequently methylated in DGC than in IGC. If methylation events are involved in the process of developing resistance against chemotherapy and radiotherapy in cancer cells, this approach may be applied to identify novel biomarkers of resistance against such cancer therapies and could aid in determining the best treatment approach for individual patients. In addition, discovery of novel methylated genes, like *PGP9.5*, will further contribute to our understanding of multiple methylation events and their roles in the biological progression of human cancers.

Acknowledgments

Received 5/2/2005; revised 9/6/2005; accepted 12/22/2005.

Grant support: National Cancer Institute grant U01-CA84986 and Oncomethylome Sciences, SA.

The costs of publication of this article were defrayed in part by the payment of page charges. This article must therefore be hereby marked *advertisement* in accordance with 18 U.S.C. Section 1734 solely to indicate this fact.

References

- Ushijima T, Sasako M. Focus on gastric cancer. *Cancer Cell* 2004;5:121–5.
- Ridley A. Molecular switches in metastasis. *Nature (Lond)* 2000;406:466–7.
- Hermanek P. Prognostic factors in stomach cancer surgery. *Eur J Surg Oncol* 1986;12:241–6.
- Wu M, Yang K, Shun C, et al. Distinct clinicopathologic characteristics of diffuse- and intestinal-type gastric cancer in Taiwan. *J Clin Gastroenterol* 1997;25:646–9.
- Yawata A, Adachi M, Okuda H, et al. Prolonged cell survival enhances peritoneal dissemination of gastric cancer cells. *Oncogene* 1998;16:2681–6.
- Kobayashi M, Nagata S, Iwasaki T, et al. Dedifferentiation of adenocarcinomas by activation of phosphatidylinositol 3-kinase. *Proc Natl Acad Sci U S A* 1999;96:4874–9.
- Ishii Y, Ochiai A, Yamada T, et al. Integrin $\alpha 6 \beta 4$ as a suppressor and a predictive marker for peritoneal dissemination in human gastric cancer. *Gastroenterology* 2000;118:497–506.
- Nishimura S, Adachi M, Ishida T, et al. Adenovirus-mediated transfection of caspase-8 augments anoikis and inhibits peritoneal dissemination of human gastric carcinoma cells. *Cancer Res* 2001;61:7009–14.
- Elster K, Carson W, Wild A, Thomasko A. Evaluation of histological classification in early gastric cancer (an analysis of 300 cases). *Endoscopy* 1979;11:203–6.
- Teh M, Lee Y. Intestinal and diffuse carcinoma of the stomach among the ethnic and dialect groups in Singapore. *Cancer* 1987;60:921–5.
- Janssen C, Jr., Maartmann-Moe H, Lie, R, Matre R.

- Age and sex distribution of intestinal and diffuse type carcinoma. *APMIS* 1991;99:78-82.
12. Zangheri G, Di Gregorio C, Sacchetti C, et al. Familial occurrence of gastric cancer in the 2-year experience of population-based registry. *Cancer* 1990;66:2047-51.
 13. Becker K, Atkinson M, Reich U, et al. E-cadherin gene mutations provide clues to diffuse type gastric carcinomas. *Cancer Res* 1994;54:3845-52.
 14. Guilford P, Hopkins J, Harraway J, et al. E-cadherin germline mutations in familial gastric cancer. *Nature* 1998;392:402-5.
 15. Machando J, Oliveira C, Carvalho R, et al. E-cadherin gene (CDH1) promoter hypermethylation as the second hit in sporadic diffuse type gastric carcinoma. *Oncogene* 2001;20:1525-8.
 16. Grady W, Willis J, Guilford P, et al. Methylation of the CDH1 promoter as the second genetic hereditary diffuse gastric cancer. *Nat Genet* 2000;26:16-7.
 17. Tamura G, Yin J, Wang S, et al. E-cadherin gene promoter hypermethylation in primary human gastric carcinomas. *J Natl Cancer Inst* 2000;92:569-73.
 18. Hoque M, Begum S, Topalogu O, et al. Quantitative detection of promoter hypermethylation of multiple genes in the tumor, urine, and serum DNA of patients with renal cancer. *Cancer Res* 2004;64:5511-7.
 19. Danmarmann R, Li C, Yoon JH, Chin PL, Bates S, Pfeifer GP. Epigenetic inactivation of a RAS association domain family protein from lung tumor suppressor locus 3p21.3. *Nat Genet* 2000;25:315-9.
 20. Yoshikawa H, Matsubara K, Qian GS, et al. SOCS-1, a negative regulator of the JAK/STAT pathway, is silenced by methylation in human hepatocellular carcinoma and shows growth suppression activity. *Nat Genet* 2001;28:29-35.
 21. Li QL, Ito K, Sakakura C, et al. Causal relationship between the loss of RUNX3 expression and gastric cancer. *Cell* 2002;109:113-24.
 22. Suzuki H, Gabrielson E, Chen W, et al. A genomic screen for genes upregulated by demethylation and histone deacetylase inhibition in human colorectal cancer. *Nat Genet* 2002;31:141-9.
 23. Yamashita K, Upadhyay S, Osada M, et al. Pharmacological unmasking of epigenetically silenced tumor suppressor genes in esophageal squamous cell carcinoma. *Cancer Cell* 2002;2:485-95.
 24. Tokumaru Y, Yamashita K, Osada M, et al. Inverse correlation between cyclin A1 hypermethylation and p53 mutation in head and neck cancer identified by reversal of epigenetic silencing. *Cancer Res* 2004;64:5982-7.
 25. Mandelker D, Yamashita K, Tokumaru Y, et al. PGP9.5 Promoter methylation is an independent prognostic factor for esophageal squamous cell carcinoma. *Cancer Res* 2005;65:4963-8.
 26. Honda T, Tamura G, Waki T, et al. Hypermethylation of the TSLC1 gene promoter in primary gastric cancers and gastric cancer cell lines. *Jpn J Cancer Res* 2002;93:857-60.
 27. Cimerman M, Repse S, Jelenc F, et al. Comparison of Lauren's, Ming's and WHO histological classifications of gastric cancer as a prognostic factor for operative patients. *Int Surg* 1994;79:27-32.
 28. Adachi Y, Yasuda K, Inomata M, et al. Pathology and prognosis of gastric carcinoma: well versus poorly differentiated type. *Cancer* 2000;89:1418-24.
 29. Rohde H, Bauer P, Stutzer H, Heitmann K, Gebbensleben B. Proximal compared with distal adenocarcinoma of the stomach: differences and consequences. German Gastric Cancer TNM Study Group. *Br J Surg* 1991;78:1242-8.
 30. Skinner J, Whitehead R. Tumor markers in carcinoma and premalignant states of the stomach in humans. *Eur J Cancer Clin Oncol* 1982;18:227-35.
 31. Fiocca R, Villani L, Tenti P, et al. The foveolar cell component of gastric cancer. *Hum Pathol* 1990;21:260-70.
 32. Teh M, Lee Y. HLA-DR antigen expression in intestinal-type and diffuse-type gastric carcinoma. *Cancer* 1992;69:1104-7.
 33. Hurlimann J, Saraga E. Expression of p53 protein in gastric carcinomas. Association with histologic type and prognosis. *Am J Surg Pathol* 1994;18:1247-53.
 34. Lin J, Wu M, Shun C, et al. Occurrence of microsatellite instability in gastric carcinoma is associated with enhanced expression of erbB2 oncoprotein. *Cancer Res* 1995;55:1428-30.
 35. Fricke E, Keller G, Becker I, et al. Relationship between E-cadherin gene mutation and p53 gene mutation, p53 accumulation, Bcl-2 expression and Ki-67 staining in diffuse type gastric carcinoma. *Int J Cancer* 2003;104:60-5.
 36. Sato N, Fukushima N, Maitra A, et al. Discovery of novel targets for aberrant methylation in pancreatic carcinoma using high-throughput microarrays. *Cancer Res* 2003;63:3735-42.
 37. Yamashita K, Minori M, Inoue H, Mori M, Sidransky D. A tumor-suppressive role for trypsin in human cancer progression. *Cancer Res* 2003;63:6575-8.
 38. Douglas D, Akiyama Y, Carraway H, et al. Hypermethylation of a small CpG-rich region correlates with loss of activator protein-2alpha expression during progression of breast cancer. *Cancer Res* 2004;64:1611-20.
 39. Oda T, Kanai Y, Oyama T, et al. E-cadherin gene mutation in human gastric carcinoma cell lines. *Proc Natl Acad Sci U S A* 1994;91:1858-62.
 40. Cameron E, Bachman K, Myohanen S, Herman J, Baylin S. Synergy of demethylation and histone deacetylase inhibition in the re-expression of genes silenced in cancers. *Nat Genet* 1999;21:103-7.
 41. Esteller M, Sanchez-Cespedes M, Rosell R, et al. Detection of aberrant promoter hypermethylation of tumor suppressor genes in serum DNA from non-small cell lung cancer patients. *Cancer Res* 1999;59:67-70.
 42. Kawakami K, Brabender J, Lord RV, et al. Hypermethylated APC DNA in plasma and prognosis of patients with esophageal adenocarcinoma. *J Natl Cancer Inst* 2000;92:1805-11.
 43. Sanchez-Cespedes M, Esteller M, Wu L, et al. Gene promoter hypermethylation in tumors and serum of head and neck cancer patients. *Cancer Res* 2000;60:892-5.
 44. Jeronimo C, Usadel H, Henrique R, et al. Quantitation of GSTP1 methylation in non-neoplastic prostatic tissue and organ-confined prostate adenocarcinoma. *J Natl Cancer Inst* 2001;93:1747-52.
 45. Usadel H, Brabender J, Danenberg KD, et al. Quantitative adenomatous polyposis coli promoter methylation analysis in tumor tissue, serum, and plasma DNA of patients with lung cancer. *Cancer Res* 2002;62:371-5.
 46. Harden S, Sanderson H, Goodman S, et al. Quantitative GSTP1 methylation and the detection of prostate adenocarcinoma in sextant biopsies. *J Natl Cancer Inst* 2003;95:1634-7.

FHIT Is Up-Regulated by Inflammatory Stimuli and Inhibits Prostaglandin E₂-Mediated Cancer Progression

Koshi Mimori,¹ Hideshi Ishii,² Hisashi Nagahara,¹ Tomoya Sudo,¹ Keishi Yamashita,¹ Hiroshi Inoue,¹ Graham F. Barnard,³ and Masaki Mori¹

¹Department of Surgical Oncology, Medical Institute of Bioregulation, Kyushu University, Beppu, Japan; ²Division of Stem Cell Regulation/Molecular Hematopoiesis, Jichi Medical School, Center for Molecular Medicine, Tochigi, Japan; and ³Department of Biochemistry and Molecular Pharmacology, University of Massachusetts Medical School, Worcester, Massachusetts

Abstract

The *FHIT* gene is known to be susceptible to environmental carcinogens. Formation of prostaglandin E₂ (PGE₂) is catalyzed by cyclooxygenase-2 (COX-2) and may influence malignant phenotype in colorectal cancer. We explored whether FHIT might play a role in progression of colorectal cancer through inflammation-associated PGE₂ activity. Immunohistochemical study of COX-2 and FHIT expression was done in 92 colorectal cancer tumors. We also used a FHIT-expressing cancer cell line (H460) induced by ponasterone A and two *FHIT* small interfering RNA-treated colorectal cancer cell lines (CCK81 and DLD1). After PGE₂ stimulation, we compared synthesis of PGE₂ (ELISA assay) and cell proliferation [3-(4,5-dimethylthiazol-2-yl)-2,5-diphenyltetrazolium bromide assay]. Immunohistochemistry showed a significant association between COX-2 and FHIT expression in colorectal cancers ($P < 0.01$). In a subset of 41 COX-2-expressing tumors, 12 FHIT⁻ tumors showed deeper cancer invasion than 29 FHIT⁺ tumors ($P < 0.01$). Experimental study, however, showed there was no direct interaction between FHIT and COX-2. Considered with results from another experiment with epidermal growth factor receptor (EGFR), we hypothesize that FHIT and COX-2 might be regulated by a common molecule, such as EGFR. Additionally, there was an inverse and direct correlation between PGE₂ synthesis and FHIT *in vitro*, suggesting that FHIT's postulated antiaggressive effect on tumor goes through PGE₂ but not COX-2. Loss of FHIT expression in colorectal cancer suggests higher malignant potential. We conclude that FHIT suppressed cancer cell proliferation in this malignancy by directly inhibiting synthesis of PGE₂ but not affecting that of COX-2. (Cancer Res 2006; 66(5): 2683-90)

Introduction

The *FHIT* gene encompasses the environmental carcinogen-sensitive common fragile site, *FRA3B*. The gene is frequently hemizygotously or homozygotously deleted in several kinds of cancers (1-5), including environmental carcinogen-related cancers, such as those of the lung (6-10) and esophagus (11). Numerous studies have reported altered *FHIT* expression not only in advanced tumors but also in precancerous lesions, suggesting that *FHIT* mutation or

deletion can be an early event in carcinogenesis (12). Abundant expression of FHIT protein has been shown to cause apoptosis in various cancer-derived cell types (13, 14), suggesting that wild-type FHIT may act as a tumor suppressor against cancer cells. We, therefore, hypothesized that *FHIT* might be a susceptible gene whose reconstitution could act against environmental carcinogens.

For a number of cancers associated with external or internal carcinogens, including colorectal cancer, inflammation is considered to be a key event affecting tissue. Prostaglandin E₂ (PGE₂) is considered to play a key role in inflammation through synthesis from arachidonic acid by cyclooxygenase-2 (COX-2). In the current study, we first investigated expression of FHIT and COX-2 with immunohistochemical techniques in 92 colorectal cancer tumors. Although we found a positive correlation between them ($P < 0.001$), there was no direct relationship in *in vitro* experiments. Then, we focused on a possible relationship between FHIT and PGE₂.

We clarified whether induction of PGE₂ in cancer cells promotes cellular proliferation and whether FHIT protein regulates PGE₂ induction. PGE₂ production and cellular proliferation were compared for cells that overexpressed FHIT and control cells that did not express FHIT, respectively. In addition, as a confirmation experiment, we compared FHIT-knocked down cells and control cells. Consequently, we discovered that FHIT inhibits PGE₂ activation directly.

Concerning the susceptible marker for colorectal cancer, we predict that loss of FHIT expression and positive expression of PGE₂/COX-2 indicate worse malignant behavior in colorectal cancer tumors. In addition, our findings suggest that delivery of FHIT protein may be a novel molecular therapy that could possibly prevent inflammation-related malignant progression.

Materials and Methods

Colorectal cancer tissue samples. A total of 92 colorectal adenocarcinomas excised at our institution and the Department of Surgery, Oita Prefectural Hospital, Oita, Japan were used after receiving approval from each institutional ethics committee and confirming that informed consent had been obtained from all subjects. Samples represented 53 male and 39 female patients with a mean age of 66 years (range, 15-88 years). None of the patients had a familial history of colorectal cancer.

Immunohistochemistry. Paraffin-embedded cancer tissue specimens and corresponding normal tissue specimens were examined by immunohistochemical analysis with COX-2 monoclonal antibody (C22420, Transduction Laboratories, San Diego, CA) and FHIT polyclonal antiserum (Zymed Laboratories, Inc., Koto-Ku, Tokyo, Japan), as previously described (11). All sections were examined independently by three investigators (K.M., Hir.I., and M.M.). We scored tumors as expression negative for COX-2 or FHIT when <10% of carcinoma cells were stained in an examined area of a specimen. Staining for COX-2 and FHIT was done on adjacent sections. All cases were examined for histologic differentiation, depth of tumor invasion,

Requests for reprints: Masaki Mori, FACS Department of Surgical Oncology, Medical Institute of Bioregulation, Kyushu University, 4546 Tsurumihara, Beppu 874-0838, Oita, Japan. Phone: 81-977-27-1650; Fax: 81-977-27-1651; E-mail: mmori@beppu.kyushu-u.ac.jp.

©2006 American Association for Cancer Research.
doi:10.1158/0008-5472.CAN-05-2509

lymphatic permeation, vascular vessel invasion, lymph node metastasis, and Duke's disease stage.

Cell culture and inducible FHIT transfectants. We transfected H460 cells with the pVgRXR vector and H460 cells with the pIND vector (control) provided by Dr. Jennifer Pietenpol (Vanderbilt University). The cells were cultured in DMEM medium with 10% fetal bovine serum (FBS), G418, and Zeocin. After administration of 10 $\mu\text{mol/L}$ ponasterone A, the ability to induce the *FHIT* transgene was confirmed by Western blot analysis. Using this clone, we compared COX-2 expression in *FHIT*⁺ cells and *FHIT*⁻ cells after lipopolysaccharide (LPS) stimulation.

Measurement of PGE₂ production by ELISA. Induction of PGE₂ synthesis by 0.1 and 1.0 $\mu\text{g/mL}$ LPS, 10 ng/mL interleukin-1 β (IL-1 β), and 10 ng/mL phorbol 12-myristate 13-acetate (PMA) was done as previously described (15) for *FHIT* transfectant and control cells.

At 24 hours after ponasterone A administration, culture medium was replaced with fresh 10% FBS medium containing 1.0 $\mu\text{g/mL}$ LPS, 10 ng/mL IL-1 β , and 10 ng/mL PMA. We did experiments four times for PGE₂-inducing stimulation and obtained each average score with SE using Student's *t* test analysis. Cells were then incubated for an additional 48 hours before PGE₂ expression was determined using the enzyme immunoassay kit-monoclonal antibody (Cayman Chemical Co., Ann Arbor, MI), according to the manufacturer's instructions.

Comparison of cell proliferation by 3-(4,5-dimethylthiazol-2-yl)-2,5-diphenyltetrazolium bromide assay. We compared proliferation rate

using an [3-(4,5-dimethylthiazol-2-yl)-2,5-diphenyltetrazolium bromide (MTT)] assay after ponasterone A administration of *FHIT*-expressing cells as well as control cells that did not express *FHIT*. Induced *FHIT* expression was initially elevated 24 hours after ponasterone A administration, and we added ponasterone A every 24 hours until 72 hours later. At 24 hours before the experiment, we initially administered ponasterone A, then we started inducing PGE₂ expression in both *FHIT*-expressing cells and control cells by stimulation with 1.0 μg LPS at 0 hour. We did all experiments four times for each stimulant; therefore, we calculated 12 data points at each time and for each cell type to calculate the average and SE. In brief, 20- μL suspensions of 2×10^4 cells treated with 1.0 $\mu\text{g/mL}$ LPS, which showed a significant difference of PGE₂ production between *FHIT*⁺ and *FHIT*⁻, were aliquoted into microtiter plate wells. The untreated cells were used as controls for nonspecific dye reduction. After incubation for 0, 4, 24, 48, or 96 hours in a humidified 5% CO₂ atmosphere, plates were spun at 700 $\times g$, the supernatants were discarded, and 20- μL MTT solution (10 $\mu\text{mol/L}$) was added to each well except for those containing nontreated controls. After an additional hour of incubation, 150 μL DMSO was added to every well to extract the formazan form of MTT. Formazan absorbance was measured at 565 nm; values are represented as absorbance per mg protein. Under LPS stimulation, increased expression of COX-2 was observed independently from *FHIT* expression (Western blotting, described below).

Selection of small interfering RNA-transfected colorectal cancer cells by quantitative real-time reverse transcription-PCR. The *FHIT* gene is encoded by 10 exons in a 1.1-kb transcript. We examined and quantified *FHIT* mRNA expression in the colorectal cancer cell lines LoVo, HT29, DLD-1, COLO320DM, COLO205, COLO201, and CCK-81 by quantitative reverse transcription-PCR (RT-PCR) assay (LightCycler 2000, Roche Diagnostics, Tokyo, Japan) using nested primers as described previously (16).

Small interfering RNA transfection. We used DLD-1 and CCK-81 cell lines, both of which express *FHIT* protein, as representative colorectal cancer cell lines. The expression vector pSilencerTM3.1-H1 hygro (Ambion, Inc., Austin, TX) was used for expression of small interfering RNA (siRNA). A hairpin siRNA designed to target the *FHIT* gene (5'-GGAAGGCUUGGAGACUUUUCATT-3', sense; 5'-UGAAAGUCUCCAGC-CUUCCTG-3', antisense) was inserted into pSilencer according to the manufacturer's instructions, and it was transfected into DLD-1 and CCK-81 cells by the LipofectAMINE method (Life Technologies, Inc., Tokyo, Japan). Two stably transfected clones were selected after hygromycin (800 $\mu\text{g/mL}$) treatment and were used for subsequent experiments. Mock empty vector transfectants of each cell line were used as controls. Inhibition of *FHIT* expression in both CCK-81 and DLD-1 was confirmed by fluorescent staining with *FHIT* antibody. Inhibition of *FHIT* with *FHIT* siRNA in CCK-81 compared with *FHIT*-expressing CCK-81 was examined by Western blotting analysis.

Western blot analysis. Cells ($5-10 \times 10^7/\text{mL}$) were washed with PBS and lysed for 20 minutes in 2 mL of 25 mmol/L Tris-HCl (pH 7.5), 150 mmol/L NaCl, 5 mmol/L EDTA, 1% Triton X-100 at 4°C. The lysate was homogenized by passing the sample through a 22-gauge needle. In brief, for immunoblot analysis, the samples were subjected to SDS-PAGE in 15% acrylamide gels under reducing conditions and transferred to Immobilon-P membranes (Millipore, Bedford, MA). After blocking with 5% nonfat dry milk and 0.05% Tween 20 in PBS, blots were incubated with COX-2 monoclonal antibody and/or *FHIT* polyclonal antiserum. After several washings, blots were incubated for 1 hour with goat antimouse IgG (1:5,000) coupled to horseradish peroxidase, washed extensively, and developed using an enhanced chemiluminescence (ECL) Western blotting kit (Amersham, Buckinghamshire, United Kingdom).

ELISA and MTT assays for colorectal cancer cells with *FHIT* siRNA. In both DLD-1 and CCK-81 cells, PGE₂ production in *FHIT*⁻ siRNA-treated cells was compared with the *FHIT*⁻ control cells by the ELISA assay described above. In addition, cell proliferation rate in *FHIT*⁻ siRNA-treated cells was compared with the rate for *FHIT*⁺ control cells using the MTT assay described above.

Epidermal growth factor receptor transfection. According to the results of the current immunohistochemical study, we disclosed concordant

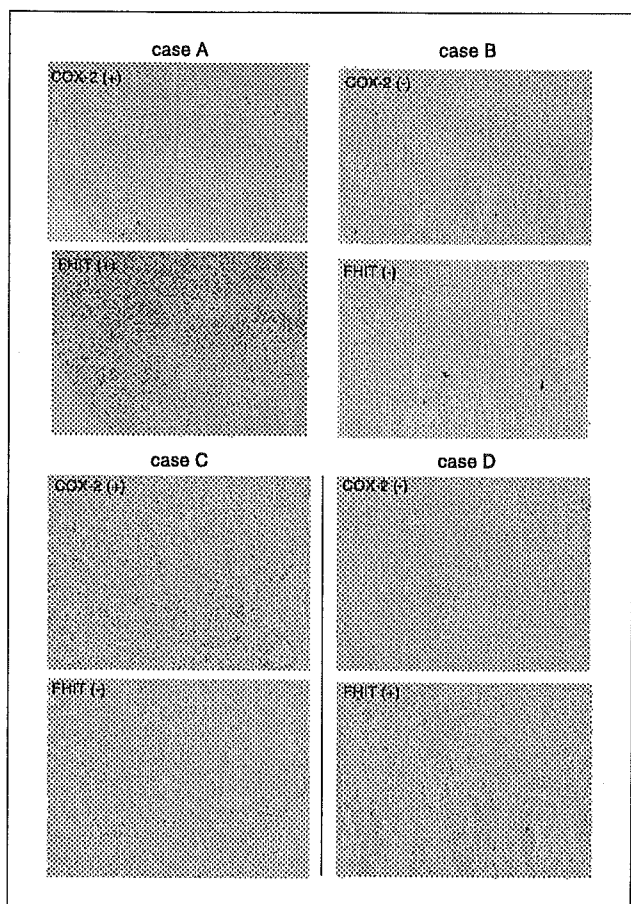


Figure 1. Immunohistochemical detection of COX-2 and *FHIT* protein in colorectal cancer cases. A, representative case of COX-2⁻ [COX(-)] and *FHIT*⁺ [*FHIT*(+)] expression. Magnification, $\times 40$. B, case with COX-2⁻ [COX(-)] and *FHIT*⁻ [*FHIT*(-)] expression. Magnification, $\times 40$. C, case with COX-2⁺ [COX(+)] but *FHIT*⁻ [*FHIT*(-)] expression. Magnification, $\times 40$. D, case with COX-2⁻ [COX(-)] but *FHIT*⁺ [*FHIT*(+)] expression. Magnification, $\times 40$.

Table 1. Clinicopathologic characteristics of COX-2 or FHIT expression in colorectal cancer

Variables	COX-2 ⁺ (n = 41)			P	COX-2 ⁻ (n = 51)			P
	n	FHIT ⁻ (n = 12)	FHIT ⁺ (n = 29)		n	FHIT ⁻ (n = 37)	FHIT ⁺ (n = 14)	
Sex								
Male (n = 53)	22	7	15	ns	31	24	7	ns
Female (n = 39)	19	5	14		31	24	7	
Histology								
Well differentiated (n = 38)	12	3	9	ns	26	18	8	ns
Moderately differentiated (n = 47)	29	9	20		18	14	4	
Poorly differentiated (n = 3)	0	0	0		3	3	0	
Others (n = 4)	0	0	0		4	2	2	
Depth of invasion								
Within muscle layer (n = 43)	17	1	16	<0.01	26	19	7	ns
Beyond subserosal layer (n = 49)	24	11	13		25	18	7	
Lymph node metastasis								
Negative (n = 51)	21	6	15	ns	30	18	12	0.02
Positive (n = 41)	20	6	14		21	19	2	
Lymph vessel permeation								
Negative (n = 50)	22	5	17	ns	28	19	9	ns
Positive (n = 42)	19	7	12		23	18	5	
Vascular vessel permeation								
Negative (n = 65)	29	7	22	ns	36	24	12	ns
Positive (n = 27)	12	5	7		15	13	2	
Distant metastasis								
Negative (n = 82)	34	8	26	ns	48	34	14	ns
Positive (n = 10)	7	4	3		3	3	0	
Duke's stage								
A, B (n = 51)	21	6	15	ns	30	18	12	0.02
C, D (n = 41)	20	6	14		21	19	2	

Abbreviation: ns, not significant.

expression of COX-2 and FHIT proteins. We assumed that epidermal growth factor receptor (EGFR) on inflammatory lesions in colorectal cancer tumors is a key molecule because a recent study reported that tobacco smoking activates EGFR signaling, thereby contributing to the elevated levels of COX-2 found in the oral mucosa of smokers (17). We prepared *EGFR* vector pLSX (provided by Prof. A Takayanagi, Keio University). Subsequent to cutting 3.9-kb *EGFR* out at the *Xho*I site from the pLSX vector, *EGFR* was inserted into the pBCKMV-hEGFR vector (Stratagene, La Jolla, CA; ref. 18).

In our previous study, we discovered mutations of the *EGFR* gene in >10% of cases of sporadic colorectal cancer (19). Considering the practical role of EGFR on inflammatory lesions, we examined alteration of COX-2 and FHIT expression in *EGFR*-mutated clones as well as *EGFR* wild-type clones. In addition to the wild-type plasmid of *EGFR*, we established mutant clones that had been discovered in human cases of sporadic colorectal cancer in our previous study. We artificially altered nucleotides at 2245 G>A (E749K) in exon 19 and 2285 A>G (E762G) and 2299 G>A (A767T) in exon 20. To establish those mutant clones, we followed the manufacturer's protocol of the QuickChange Site-Directed Mutagenesis kit (Stratagene). Those mutant plasmids were inserted into the expression vector, and subcloning was done. We considered the *EGFR* (wild-type)-inserted plasmid without expression of the gene as a "mock" clone.

For transfection, 6×10^4 COLO205 cells were seeded in DMEM with 10% FCS on six-well culture plates. After 24 hours, medium was exchanged with 2 mL DMEM supplemented with 0.2% FCS and cultured for an additional 4 hours. Transfection was done using LipofectAMINE 2000 (Invitrogen, Carlsbad, CA), according to the manufacturer's instructions, with minor modifications. Briefly, 5 µg plasmid DNA purified by an endotoxin-free

purification system (Qiagen, Tokyo, Japan) were diluted in 50 µL serum-free DMEM. The diluted DNA was mixed with 4 µL reagent, which was prediluted in 50 µL serum-free DMEM. The mixture of DNA and reagent was added to the culture medium in a dropwise manner. Two-milliliter DMEM with 20% FCS was added to the culture medium. Cells were grown for 48 hours and subjected to protein study.

Immunoblot. Cells with wild-type *EGFR* and mutant clone-transfected cells were harvested, washed with PBS, and homogenized in lysis buffer containing 1 mmol/L Tris-HCl, 2 mmol/L EDTA, 100 mmol/L NaCl, 1% NP40, 1% Triton X-100, 10 mmol/L sodium orthovanadate, 5% leupeptine,

Table 2. Relationship between FHIT and COX-2 protein expression

	COX-2 protein expression		P
	Positive (n = 41)	Negative (n = 51)	
FHIT protein expression			
Positive (n = 43)	29	14	<0.01
Negative (n = 49)	12	37	

NOTE: A significant association was observed between FHIT expression and COX-2 expression ($P < 0.001$).

and 5 mmol/L phenylmethylsulfonyl fluoride with complete proteinase inhibitor cocktail (Sigma-Aldrich, Tokyo, Japan). After samples were centrifuged for 10 minutes at $9,000 \times g$ at 4°C , the supernatant was used for immunoblot analysis. After assessment of protein concentration using the protein assay kit (Bio-Rad, Tokyo, Japan), 15 μg protein was mixed with SDS-sample buffer (Bio-Rad), boiled, and loaded in 5% to 20% gradient SDS-PAGE gel (Bio-Rad). Separated proteins were electrotransferred to a polyvinylidene difluoride membrane (AMRESCO, Solon, OH). The membrane was blocked with 2.5% skim milk and 2.5% bovine serum albumin in TBS supplemented with 0.1% Tween 20, stained at 4°C overnight with primary mouse monoclonal antibodies, anti-EGFR (BD Transduction Laboratory, Franklin Lakes, NJ) at 1:500 dilution, COX-2 at 1:500 dilution, and actin at 1:3,000 dilution, or rabbit polyclonal anti-FHIT antibody at 1:1,000 dilution, washed, stained at 22°C for 2 hours with secondary antibodies (Amersham, Piscataway, NJ), and visualized on film by the ECL-plus system (Amersham). Expression of EGFR, FHIT, and COX-2 proteins were adjusted by actin expression and were calculated by NIH Image ver.1.62.

Statistical evaluation. Associations among protein expression and clinicopathologic variables were computed using either the two-tailed χ^2

test or Fisher's exact test, as appropriate. A comparison of PGE₂ production by ELISA between FHIT-expressing and nonexpressing cells was calculated by Student's *t* test. Cell proliferation as evaluated by mean absorbance was compared between FHIT⁺ and FHIT⁻ cells, and the average at each elapsed time was also calculated by Student's *t* test. *P* < 0.05 was considered statistically significant. In Western blotting of EGFR transfectants, linear regression analysis was applied to the relationship between EGFR and COX-2 and the relationship between EGFR and FHIT.

Results

Immunohistochemical analysis of FHIT and COX-2 in colorectal cancer tumors. We found that COX-2 was overexpressed in cancerous and surrounding noncancerous cells in samples obtained from colorectal cancer resections, whereas adenoma samples showed substantial COX-2 expression in interstitial tissue (data not shown) consistent with a previous report (20). We evaluated COX-2 and FHIT expression in adenocarcinomas of the colon and rectum (Fig. 1). Analysis of

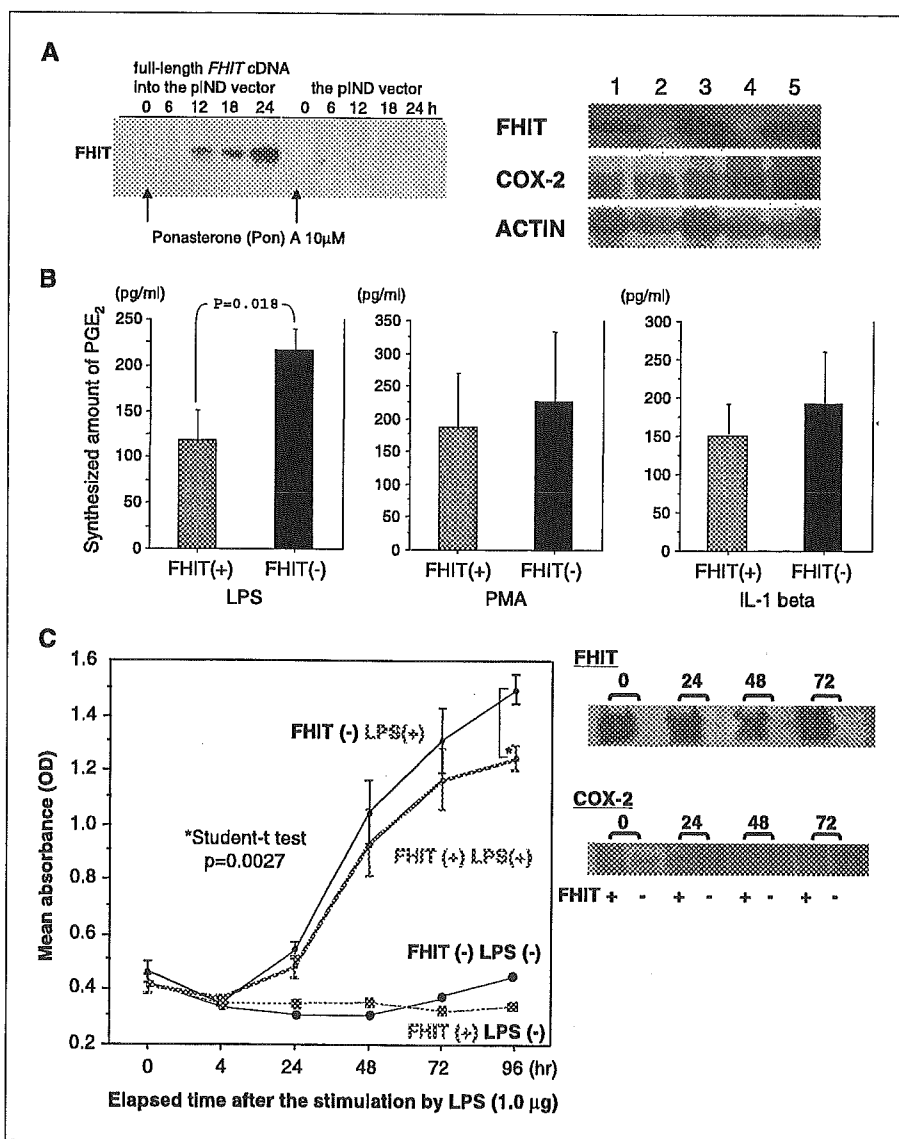


Figure 2. Induction of FHIT inhibits PGE₂ production and cell proliferation activated by stimulation of an inflammation-associated pathway. **A**, Western blot of FHIT-inducible H460 transfectants after exposure to ponasterone (Pon) A as inducer. *Left*, after addition of ponasterone A (10 $\mu\text{mol/L}$) to the medium, FHIT-inducible transfectants with full-length FHIT cDNA in pIND vector and control transfectants with empty pIND vector were subjected to Western blot with anti-FHIT antiserum. Clear induction was observed in FHIT-inducible cells, whereas no expression was detected in the control. *Right*, Western blot was performed to assess COX-2 expression between FHIT-inducible cells (lanes 1, 3, and 5) and empty vector control cells (lanes 2 and 4) after exposure to 10 $\mu\text{mol/L}$ ponasterone A for 24 hours. Increasing amounts of LPS were added to the medium and cultured for an additional 72 hours (final LPS concentration: lane 1, 0.1 $\mu\text{g/mL}$; lanes 2 and 3, 0.5 $\mu\text{g/mL}$; lanes 4 and 5, 1.0 $\mu\text{g/mL}$). The medium was exchanged every 24 hours with fresh medium containing those reagents. COX-2 expression increased in an LPS dose-dependent manner, although not relevant with FHIT induction. **B**, ELISA assay of PGE₂ production. FHIT-inducible H460 cells [FHIT(+)] and control empty vector transfectants [FHIT(-)] were cultured in medium with ponasterone A for 24 hours and subjected to ELISA assay after stimulation with 1.0 $\mu\text{g/mL}$ LPS (*left*), 10 ng/mL PMA (*middle*), and 10 ng/mL IL-1 β (*right*). Four independent experiments were done to confirm reproducibility. Representative data. LPS stimulation led to an apparent difference between FHIT⁺ cells and FHIT⁻ cells under the test conditions. **C**, MTT cell proliferation assay (*left*) and protein study (*right*). FHIT-inducible H460 cells [FHIT(+)] and control empty vector transfectants [FHIT(-)] were cultured in medium with ponasterone A for 24 hours and cultured with addition of 1.0 $\mu\text{g/mL}$ LPS for indicated time, then subjected to the MTT assay. Similarly, expression of FHIT and COX-2 was assessed by Western blot at indicated time. Increased COX-2 expression was detected, whereas alterations of FHIT expression were not apparent.

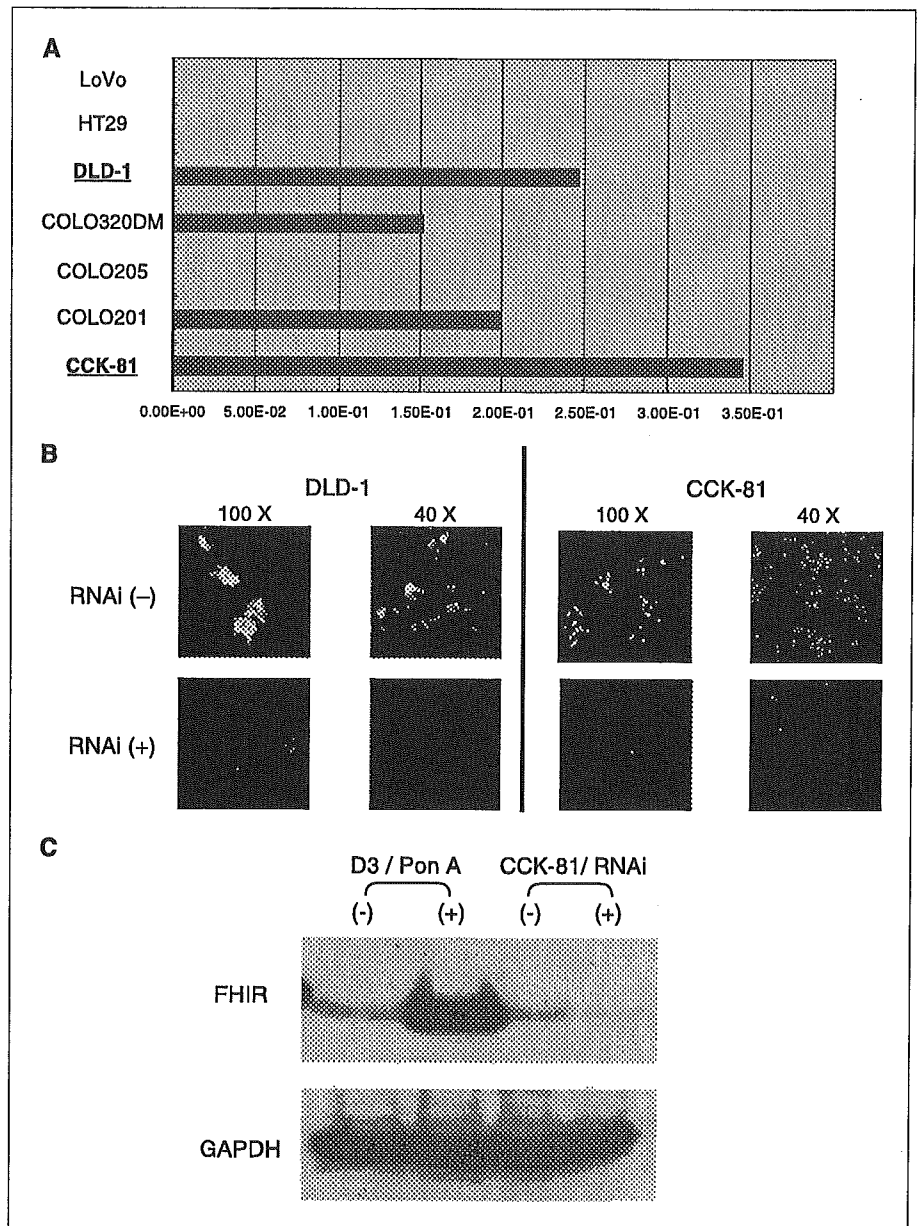


Figure 3. siRNA knock-down of FHIT. *A*, quantitative real-time RT-PCR. RNA was extracted from seven cell lines, and FHIT expression was evaluated by quantitative real-time RT-PCR. Endogenous FHIT was expressed substantially in CCK-81 cells and, to a lesser extent, in DLD-1 cells. *X-axis*, relative expression. *B*, confocal microscope observation at indicated magnifications. Fluorescence staining of FHIT protein in CCK81 and DLD-1 cells shows reduction of FHIT expression by siRNA knock-down [RNAi(+)] but not by control mock-treated cells [RNAi(-)]. *C*, Western blotting analysis. Protein was extracted from FHIT-inducible transfectant clone D3 before and after ponasterone A induction, as well as from siRNA knock-down and control mock-treated CCK-81 cells, then subjected to blotting with indicated antibodies.

clinicopathologic features of our sample of colorectal cancer cases revealed that COX-2⁺ tumors with FHIT⁻ expression showed more advanced malignant features. As shown in Table 1, among the COX-2⁺ cases, 11 of 12 (91.7%) cases of FHIT⁻ colorectal cancer invaded beyond the subserosal layer, whereas more than half of the 29 cases of FHIT⁺ colorectal cancer had invasion restricted within the muscular layer. Thus, depth of tumor invasion was more advanced in FHIT⁻/COX-2⁺ cases. In addition, among the 51 COX-2⁻ cases, disease stage was either Duke's A or B in 12 of 14 (86%) FHIT⁺ cases; this means that these cases showed a relatively early stage of disease. Table 2 shows the relationship between FHIT and COX-2 expression; there is a significant association with each other ($P < 0.001$). Two thirds (29 of 43, 67%) of the FHIT⁺ cases were also COX-2⁺, whereas 37 of the 49 (76%) FHIT⁻ cases were COX-2⁻.

COX-2 expression is not altered by FHIT expression. As shown Fig. 2A (left), induction of FHIT expression was successful. COX-2 expression increased in line with elevation in LPS concentration; however, expression of COX-2 was not affected by FHIT expression, which was regulated by ponasterone A (Fig. 2A, right). Expression of both genes was independent of the other.

Overexpression of FHIT suppresses PGE₂ synthesis. PGE₂ production was significantly inhibited in FHIT transfectants treated with ponasterone A compared with vector-only transfectant (FHIT⁻) cells treated with ponasterone A. Compared with FHIT⁻ cells, exposure of FHIT⁺ cells to LPS, IL-1 β , or PMA suppressed PGE₂ production (Fig. 2B). Thus, the averages \pm SE of PGE₂ production after LPS stimulation in FHIT⁺ cells and FHIT⁻ cells were 119.250 \pm 33.09 and 216.39 \pm 22.62, respectively. After PMA stimulation, averages were 152.26 \pm 39.44 and 192.67 \pm 67.37,